Elsevier Editorial System(tm) for Journal of Manufacturing Processes
Manuscript Draft

Manuscript Number:

Title: Thermo-mechanical characterization of Friction Stir Spot Welded AA6060 sheets: experimental and FEM analysis

Article Type: Full Length Article

Keywords: FSSW, process parameters, temperature distribution, welding force, mechanical properties, FEM simulation

Corresponding Author: Dr. Gianluca Danilo D'Urso, Ph.D.

Corresponding Author's Institution: University of Bergamo

First Author: Gianluca Danilo D'Urso, Ph.D.

Order of Authors: Gianluca Danilo D'Urso, Ph.D.

Abstract: A study was carried out to evaluate how the Friction Stir Spot Welding process parameters affect the temperature distribution in the welding region, the welding forces and the mechanical properties of the joints. An experimental campaign was performed by means of a CNC machine tool and FSSW lap joints on AA6060-T6 aluminum alloy plates were obtained. Five thermocouples were inserted into the samples to measure the temperatures during the tool plunging. A set of tests was carried out by varying the process parameters, namely rotational speed, axial feed rate, plunging depth and dwell time. Axial welding forces were measured during the execution of the experiments by means of a piezoelectric load cell. The mechanical properties of the joints were assessed by executing shear tests on the specimens. A correlation between process parameters and joints properties was found. The experimental data collected were also used to set up and to validate a simulative model of the process. The peculiarity of the developed FEM model is a 2D approach used for the simulation of a 3D problem, in order to guarantee a very simple and practical model able to achieve results in a very short time. The 2D FEM model, based on a specific external routine for the calculation of the developed thermal energy, due to the friction between tool and workpiece, was set up using the commercial code Deform 2D. An index for the prediction of the joint shear resistance using FEM simulations was finally proposed and validated.

Suggested Reviewers: Elisabetta Ceretti Prof.
University of Brescia - Italy
elisabetta.ceretti@unibs.it

Marion Merklein Prof.
Friedrich-Alexander Universität Erlangen-Nürnberg
marion.merklein@fau.de

Carlo Bruni Dr.
Università Politecnica delle Marche - Italy
c.bruni@univpm.it

Opposed Reviewers:

Cover Letter

To the Publisher of "The Journal of Manufacturing Processes"

Object: submission of a paper

Dear prof. Kapoor,

I would like to submit to the Journal of Manufacturing Processes the paper titled "Thermo-mechanical characterization of Friction Stir Spot Welded AA6060 sheets: experimental and FEM analysis".

Authors:

G. D'Urso

University of Bergamo – Dept. of Engineering – Viale Marconi 5, 24044 Dalmine (BG) - Italy – durso@unibg.it

Corresponding Author:

Gianluca D'Urso

University of Bergamo – Dept. of Engineering

Viale Marconi 5, 24044 Dalmine (BG), Italy

durso@unibg.it

tel: +39 035 2052330

mob: +39 3386093599

fax: +39 035 2052043

Paper findings and significance

In this work a study was carried out to evaluate how the Friction Stir Spot Welding process parameters affect the temperature distribution in the welding region, the welding forces and the mechanical properties of the joints. A set of tests was carried out by varying the process parameters, namely rotational speed, axial feed rate, plunging depth and dwell time.

The mechanical properties of the joints were assessed by executing shear tests on the specimens.

A dependency of welding forces and maximum achieved temperature on rotational speed and feed rate was observed: high values of rotational speed and low values of feed rate lead to lower welding forces and higher welding temperatures. In particular, the shear resistance of the joints reaches an optimum for intermediate conditions of temperature and welding forces, when the material temperature and pressure reach the condition for solid state phenomena occurrence. An increase of the shear resistance can be observed for increasing values of plunging depth and dwell time.

The experimental data collected were also used to set up and to validate a simulative model of the process. The peculiarity of the developed FEM model is a 2D approach used for the simulation of a 3D problem, in order to guarantee a very simple and practical model able to achieve results in a very short time. An index for the prediction of the joint shear resistance using FEM simulations, basing on the mean stress and the joining temperature, was finally proposed and validated.

Sincerely,

Gianluca D'Urso

Highlights

- Mechanical properties of the joints strictly related to rotational speed: optimal conditions for intermediate values
- Mechanical properties decrease for high feed rate and increase for low plunging depth and dwell time
- Optimal mechanical properties for intermediate conditions of welding temperature and forces
- The proposed FEM model well predict welding forces and temperature
- Prediction of the joint resistance using FEM simulations, basing on mean stress and temperature

Thermo-mechanical characterization of Friction Stir Spot Welded AA6060 sheets: experimental and FEM analysis

G. D'Urso

University of Bergamo – Department of Engineering – Viale Marconi 5, 24044 Dalmine (BG) - Italy – durso@unibg.it - +39 3386093599 - +39 0352052330

Keywords: FSSW, process parameters, temperature distribution, welding force, mechanical properties, FEM simulation.

Abstract

A study was carried out to evaluate how the Friction Stir Spot Welding process parameters affect the temperature distribution in the welding region, the welding forces and the mechanical properties of the joints. An experimental campaign was performed by means of a CNC machine tool and FSSW lap joints on AA6060-T6 aluminum alloy plates were obtained. Five thermocouples were inserted into the samples to measure the temperatures during the tool plunging. A set of tests was carried out by varying the process parameters, namely rotational speed, axial feed rate, plunging depth and dwell time. Axial welding forces were measured during the execution of the experiments by means of a piezoelectric load cell. The mechanical properties of the joints were assessed by executing shear tests on the specimens. A correlation between process parameters and joints properties was found.

The experimental data collected were also used to set up and to validate a simulative model of the process. The peculiarity of the developed FEM model is a 2D approach used for the simulation of a 3D problem, in order to guarantee a very simple and practical model able to achieve results in a very short time. The 2D FEM model, based on a specific external routine for the calculation of the developed thermal energy, due to the friction between tool and workpiece, was set up using the

commercial code Deform 2D. An index for the prediction of the joint shear resistance using FEM simulations was finally proposed and validated.

1. Introduction

Friction stir welding is a well-known solid state joining process developed by The Welding Institute (TWI) in Cambridge UK and patented in 1991 [1,2]. FSSW (Friction Stir Spot Welding) is a variant of the linear FSW, developed by Mazda Motor Corporation (Sakano et al. [3]) and Kawasaki Heavy Industry (Iwashita [4]). This welding technology is suitable to obtain spot lap joints and consists in a process similar to the FSW, except for the tool movement: the rotating tool is plunged into the overlapped sheets up to a predetermined depth, the rotating tool is held in that position for a specific time (often named dwell period or dwell time) and finally it is retracted. Several variations of the process also include a limited horizontal movement of the tool. The frictional heat generated at the interface between tool and workpiece softens the surrounding material, while the movement of the pin yield the material flow in both the circumferential and the axial directions [5]. The mixing of the plasticized material and the pressure applied by the tool shoulder result in the formation of a solid bond region [6]. FSSW can be considered as a transient process due to its short cycle time (usually a few seconds). During FSSW, the process parameters determine the amount of generated heat, the material plasticization around the pin, the weld geometry and therefore the mechanical properties of the joint [7].

FSSW is already applied in several industrial fields as a valid alternative to other spot joining technologies such as riveting, resistance spot welding (RSW) etc. In particular, this technology has recently received large consideration from automotive, aerospace, in-white and other industries. Such innovative techniques also allow to join the so-called un-weldable or hard-to-weld light alloys or advanced high-strength steels (AHSS) [8, 9]. Moreover, this technology can be applied to join non-metallic materials, such as polymers [10, 11]. A disadvantage of this technology is that a

keyhole generally remains at the center of the stirred zone, if a retractable pin technology is not used.

Heat and plastic flow, due to tool rotation, determine remarkable microstructural modifications resulting in a local change of material mechanical characteristics around the joint. In particular, moving from the periphery of the joint towards the joint axis, the base material (BM), in which no metallurgical modification are expected, is initially found. Then, there is a heat affected zone (HAZ), where the material undergoes a thermal load that modifies microstructure and mechanical properties. Afterwards, a thermo-mechanically affected zone (TMAZ) can be observed, in which the material is plastically deformed by the tool stirring action and an increase of the material average grain size is expected. Finally, the nugget is located in the middle of the joint, in this recrystallized area original grains are usually replaced with fine grains of uniform size [12, 13].

Furthermore, FSSW joints show a particular configuration: the tip of the notch at the surfaces in contact between the welded plates is curled upward. This effect is caused by the material flow during welding and it is commonly defined hooking effect or hook [14-16]. This hook is due to the upward bending of the initial sheets interface after penetration of the tool in the lower plate and its presence is considered a major concern when discussing the fracture of friction stir spots welds [17]. The oxide layer initially localized on the surfaces of the sheets is broken during welding and distributed through the weld, so affecting the joint resistance.

As already said, the quality of the FSSW joints depends on several process and geometrical parameters; the process parameters are spindle rotational speed, axial feed rate, dwell time and plunge depth, while the geometrical parameters are shape and diameter of both tool pin and shoulder. If process conditions for the welds are not optimized, the resulting joint may be not effective or even contain weld defects. The increasing application for this welding technology has attracted attention and interest of many researchers who have studied several aspects, such as the determination of optimal sets of process parameters, the mechanical strength and the microstructural properties of the joints, that in many cases show a reciprocal dependence.

Some Authors demonstrated that the lap shear load first increased, and then decreased for increasing values of the tool rotation speed [3, 18]. Other Authors observed that higher weld strength can be related to a larger stir zone size, achieved by reducing the tool rotation speed [19 20]. In [21] it was found that the shearing resistance of the weld increases for decreasing values of the tool rotating speed and for increasing tool plunge rate. In [20] it was declared that the weld lap shear strength can be increased by increasing the dwell time or by optimizing this parameter, as reported in [22]. On the opposite, some Authors [23] found that the resistance of the joints decreases when decreasing the tool rotating speed.

As demonstrated by the literature cited above, the results on how the process parameters affect the joint properties are diverse and the influence of the welding conditions on the joint characteristics and fracture is not yet fully understood; then, only a general comparison can be achieved because of different alloy use, varied alloy thickness and tool design.

A potential valid method to deepen some aspects concerning the thermo mechanical phenomena occurring during FSSW is based on the simulation of the process by means of FE codes.

Many investigators have tried to simulate friction stir welding process even though the use of FEA methods in this field is not widespread because, in general, it is an hard task, due to the high strain and strain rate occurring during the process, resulting in a complicated problem involving non-linear material behavior, excessive mesh distortion and high computational efforts. Moreover a validation based on the experimental measure of temperature and welding forces is always essential.

Some three-dimensional models have been developed for friction stir spot welding (FSSW) using different approaches and FEM codes. A computational fluid dynamics (CFD) approach was used by Gerlich et al. [24] to model FSSW. Using the same approach, the temperature distribution and the flow of metals, by using the computational fluid dynamic code FLUENT with non-Newtonian fluid model, was analyzed by Langerman and Kvalvik [25] and by Colegrove and Shercliff [26]. In general, when a fluid model is used, it is difficult to approximate metal properties of the plastic deformation behavior. On the other hand, in [27], the thermo-mechanical processes during the

plunge phase was analyzed by means of numerical simulation and the model was set up by using a rigid welding tool and a deformable work-piece, meshed using eight node-coupled temperature displacement brick elements. In [28], temperature, stress and temperature-deformation aspects were analyzed for aluminum alloy AA6061-T6 workpieces; adaptive meshing, which uses brick elements and allows to preserve mesh quality under high strain conditions, is used to simulate material flow and temperature distribution in FSSW process. Rajamanickam et al. [29] and Zhang and Zhang [30] analyzed the temperature distribution and the plastic deformation by using the finite element code ABAQUS with an elastic–plastic deformation model. D'Urso et al [31] set up a 3D rigid-plastic model by using DEFORM to analyze welding force and temperature distribution as a function of the process conditions.

The present work deals with an experimental and simulative study of the FSSW process for the lap-joining of thin aluminum sheets. An experimental campaign was performed on AA6060-T6 aluminum sheets. The FSSW process was applied on couples of overlapped sheets by varying rotational speed, feed rate, plunging depth and dwell time. Axial welding forces and temperature distribution in the joining region were recorded during the tests and their dependency from the welding parameters was studied. Shear tests were also performed to evaluate the quality of the joints as function of the welding conditions. The results were used to feed a simulative FEM model for the prediction of temperature distribution and welding forces. A numerical model of the FSSW process was developed and implemented using the commercial FEM code Deform 2D. A final comparison between numerical and experimental results was performed to validate the model.

2. Experimental procedure

2.1 Experimental set up

A Friction Stir Spot Welding (FSSW) experimental campaign was performed by means of a CNC machine tool. FSSW lap joints were executed on AA6060-T6 aluminum alloy sheets having a

thickness equal to 2 mm. The tool was fabricated using AISI 1040 steel, shoulder and pin diameters were respectively equal to 12 and 4 mm. Two different experimental investigations were performed to evaluate how the welding process parameters affect the thermal distribution in the welding region, the welding forces and the mechanical properties of the joints.

2.2 Thermal characterization and welding forces

The specimens used for these tests were made as single parts, by milling a plate with an initial thickness equal to 4 mm. The geometry and the dimension of the specimens are shown in figure 1. This solution was set up to avoid possible effects due to the thermal contact resistance between the plates and to guarantee proper and stable measurements of the temperatures during the tests. Five holes having a diameter equal to 1 mm were executed on each sample, in the width direction, at a specific distance from the specimen center (4, 5, 7, 8, 10 mm). These holes were carried out at half height of the overlapped part of the samples (2 mm) and their depth was equal to half of the specimens width (15 mm). Five thermocouples having a diameter equal to 1 mm were inserted into the holes during the execution of the FSSW experiments. A specific clamping system was fabricated to block the specimens and several thin rectangular slots were machined to allow the thermocouples entrance (figure 2). A Kistler piezoelectric load cell was used to measure the welding forces in axial (Z) direction. The tests were carried out varying tool rotational speed (S) [rpm], feed rate (F) [mm/min], plunging depth (Z) [mm] and dwell time (t) [s]. The tests were based on a Box-Behnken Design (factors: 4, replicates: 1, base runs: 27, total runs: 27, center points: 3). All the welding conditions are resumed in table 1.

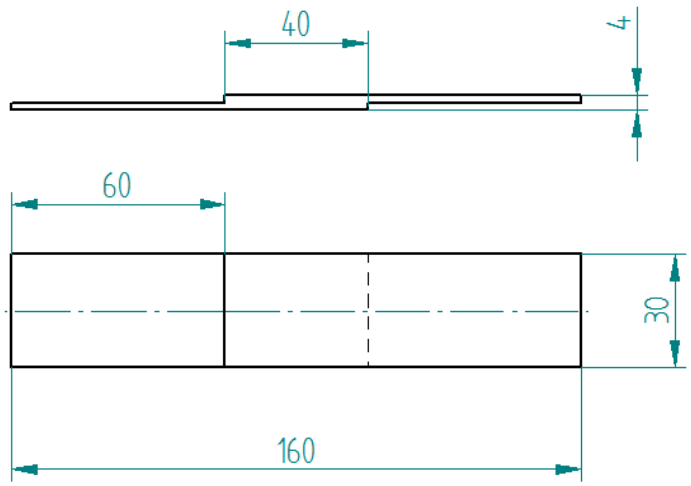

Figure 1 - Details of the specimens prepared for the thermal analysis.

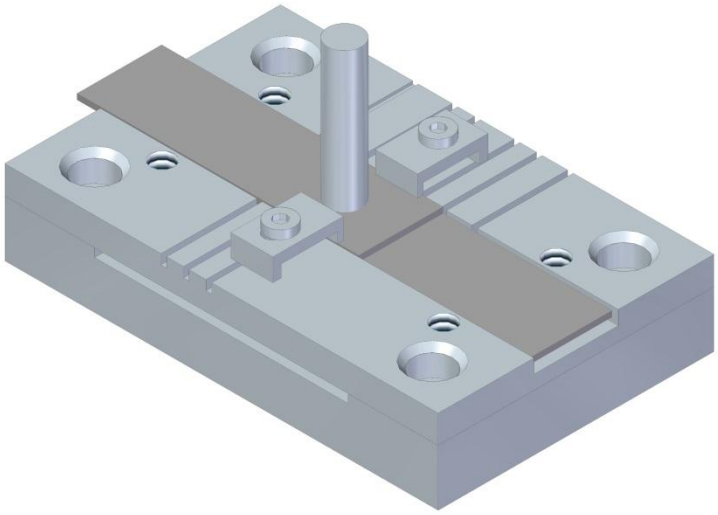

Figure 2 - Details of the clamping system.

Table 1. Welding conditions for the thermal analysis experiments.

Rotational Speed (S) [Rpm]	Feed Rate (F) [mm/min]	Plunging Depth (Z) [mm]	Dwell Time (t) [s]
1000	30	3.7	1.0
1000	20	3.7	1.5
5000	10	3.7	1.0
3000	20	3.8	0.5

5000	30	3.7	1.0
3000	30	3.7	1.5
3000	20	3.7	1.0
1000	20	3.6	1.0
3000	10	3.7	1.5
5000	20	3.8	1.0
1000	20	3.7	0.5
3000	20	3.7	1.0
3000	10	3.8	1.0
3000	30	3.8	1.0
3000	10	3.7	0.5
3000	20	3.8	1.5
5000	20	3.7	1.5
5000	20	3.7	0.5
3000	20	3.7	1.0
1000	20	3.8	1.0
1000	10	3.7	1.0
3000	20	3.6	1.5
3000	30	3.6	1.0
3000	30	3.7	0.5
3000	10	3.6	1.0
5000	20	3.6	1.0
3000	20	3.6	0.5

2.3 Mechanical characterization

Sheets having a length of 100 mm, a thickness of 2 mm and a width of 30 mm were overlapped for 40 mm and friction stir spot welded. Also in this case, the tests were carried out by varying S, F, Z and t. The experiments were based on a Multilevel Factorial Design (factors: 4, replicates: 2, base runs: 72, total runs: 144, number of levels: 4; 3; 3; 2). The values of the varied parameters are reported in table 2.

Table 2. Values of the parameters varied in the experiments for the mechanical characterization.

Rotational Speed (S) [Rpm]	Feed Rate (F) [mm/min]	Plunging Depth (Z) [mm]	Dwell Time (t) [s]
500 – 1000 – 3000 – 6000	10 – 20 - 30	3.6 – 3.7 – 3.8	0.5 – 1.5

The mechanical properties of the joints were evaluated by means of shear tests. A universal testing machine Galdabini (50 kN load cell) was used for this purpose. The traverse rate was set equal to 5 mm/min and a preload equal to 100 N was applied. The mechanical properties of the welded joints were investigated along a direction orthogonal with respect to the overlapping line. Two plates having a thickness equal to 2 mm were fixed on the edges of the specimens to avoid possible parasite bending moments. Figure 3 shows the shear test set up.

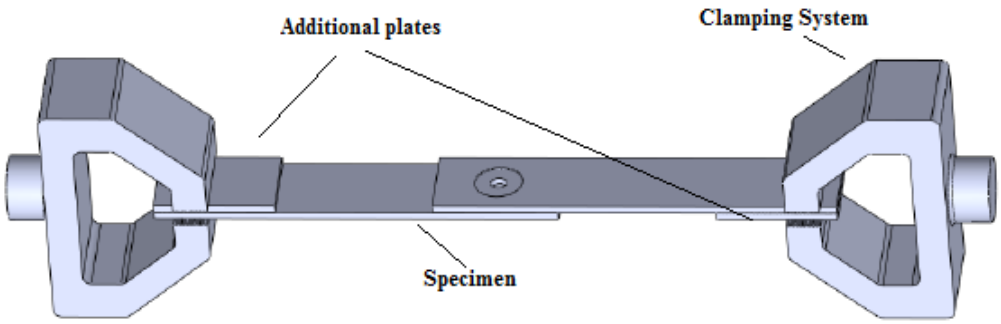

Figure 3 - Example of the shear test set up.

3. Analysis of the results

3.1 Welding forces and temperature

The Analysis of Variance (ANOVA) was carried out on the maximum values of data coming from the thermal and welding force tests. A general good repeatability with low data scatter was observed

in all cases. The main results, reported in table 3, show that welding force and temperature are influenced by both rotational speed (S) and feed rate (F), being the p-values very low (less than the alpha value set to 0.05). A partial influence can be ascribed to plunging depth (Z), while dwell time (s) resulted to not influence significantly the considered output parameters. A second degree effect on welding force, related to rotational speed, was also evidenced by the ANOVA. Based on these considerations, only the parameters that resulted to be significant were taken into account in the further analysis.

Table 3. ANOVA output for welding forces and temperature indicators.

	P-value					
Source	Welding force	T1	T2	T3	T4	T5
S	0	0	0	0	0	0
F	0	0	0	0.022	0.027	0.006
Z	0.036			> 0.05		
t	> 0.05			> 0.05		
S*S	0			> 0.05		

As an example, the regression equation of the temperature distribution for T1 (temperature measured by the thermocouple located at 4 mm from the joint axis, that is in all cases the maximum revealed temperature), is reported in eq. 1 as a function of all the parameters resulting effective from the analysis.

$$T1 = 318 + 0.0718\ S - 1.38\ F \quad (1)$$

The temperature distribution [C°], measured by the thermocouples T1 and T3, is reported in figure 4 as a function of S and F. A systematic behavior can be observed in the thermal distribution: a more sharp and higher peak of temperature is measured for low values of feed rate (at the same rotational speed). For high rotational speed the raise of temperature is faster with respect to the

lower speeds. Finally, for low values of feed rate, the temperature distribution at the initial phase of the process results very similar independently by the thermocouple position (first part of the curves continuous and dashed almost overlapped); on the contrary, for high values of the feed rate, the thermal distribution retard leads to an overlapping of the curves in the last phase of the process.

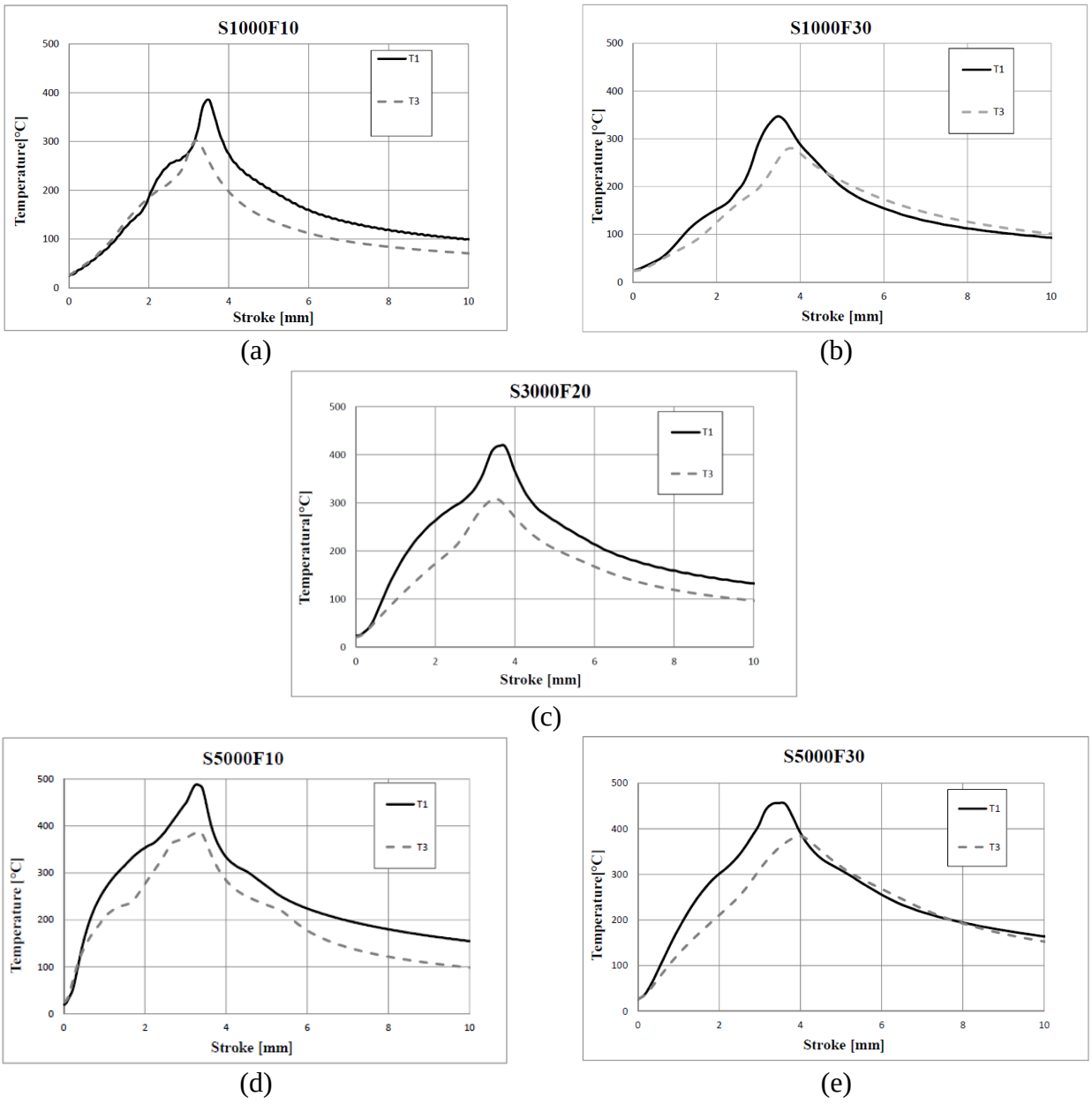

Figure 4 – Temperature distribution [C°] as a function of S and F, measured by the thermocouples T1 and T3.

Figure 5 shows the maximum temperature (at five different distances from the joint axis) and the maximum axial welding load as a function of tool rotational speed (S). The temperature values refer to an intermediate value of feed rate (F=20 mm/min). Figure 6 shows the temperature and the axial welding load as a function of feed rate (F) for an intermediate value of rotational speed (S=3000 rpm). Figure 7 shows the temperature and the axial welding load as a function of the plunging depth (Z) for intermediate values of rotational speed (S=3000 rpm) and feed rate (F=20 mm/min). As a general remark, the temperature increases for increasing values of rotational speed, while slightly decreases for increasing values of feed rate. The welding forces decrease for increasing values of rotational speed, while they increase when feed rate increases too. Finally, the maximum welding forces usually increase for deeper values of tool penetration. As a general consideration, the increase of rotational speed and the consequent higher thermo-mechanical contribution leads to an increase of the material temperature; this gives rise to the reduction of material penetration resistance and then to the reduction of axial welding force. On the contrary, the increase in welding speed accelerates the entire welding process, reducing the time in which the thermal distribution between tool and workpiece and within the workpiece itself occur; these conditions limit the temperature increase that results in higher welding force.

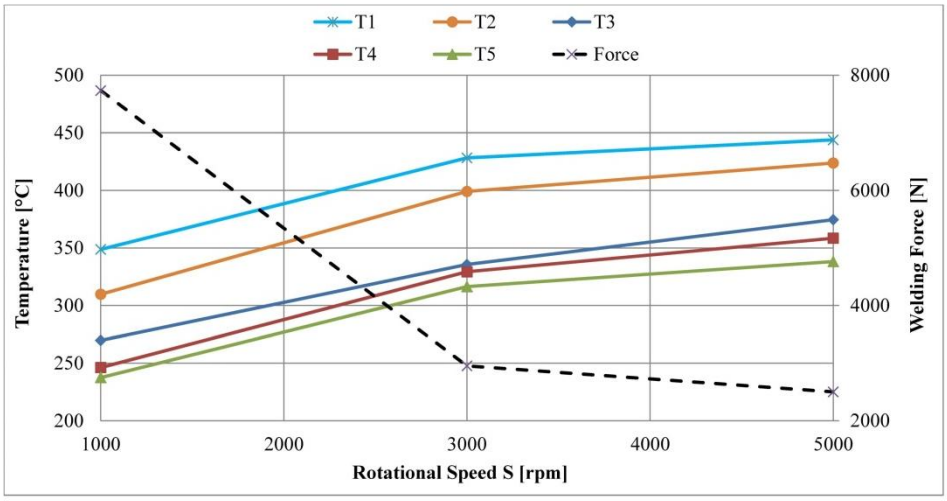

Figure 5 - Temperature and axial welding load as a function of tool rotational speed (S)

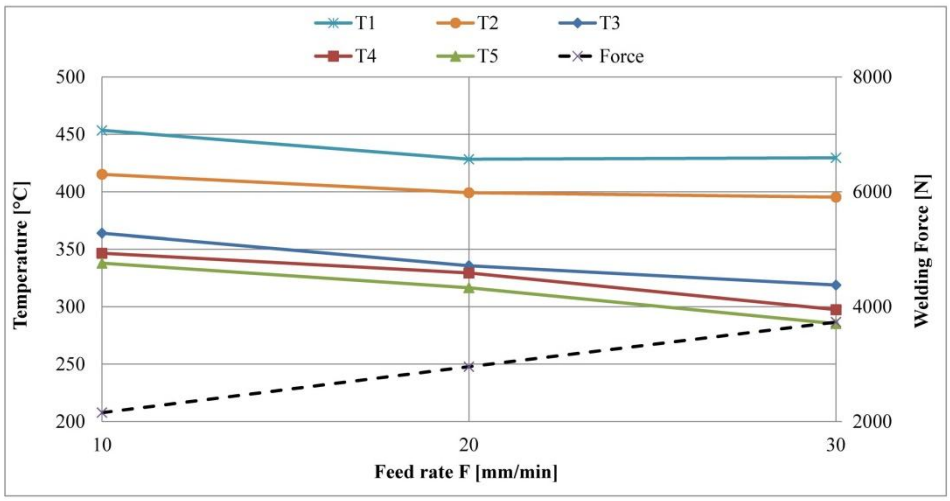

Figure 6 - Temperature and axial welding load as a function of feed rate (F)

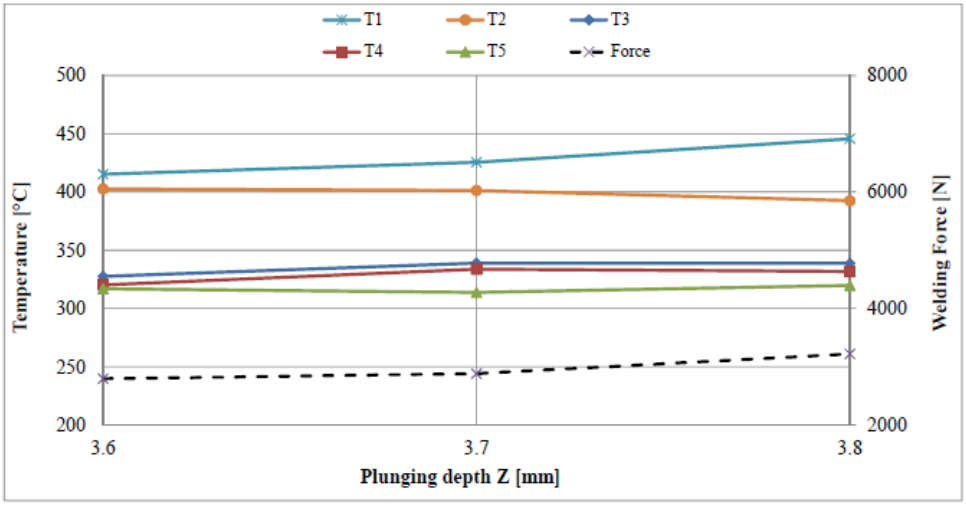

Figure 7 - Temperature and axial welding load as a function of plunging depth (Z)

In order to give a more concise representation of the results, figure 8 shows both welding force and maximum temperature data as a function of the F/S (feed rate divided by rotational speed) ratio, that represents the feed rate per unit revolution [mm/rev]. In effect, this parameter is strictly related to the thermal contribution. The data concerning plunging depth and dwell time were averaged since considered as not significant from the ANOVA analysis.

As a general conclusion, it is possible to state that high values of rotational speed and low values of feed rate lead to high welding temperatures and low welding forces. An opposite result can be obtained by means of high rotational speed and low feed rate. This effect can be related to the thermal contribution which in general increases for decreasing values of the ratio between F and S. Anyway, some more considerations can be drawn taking into account also the results of the mechanical tests reported in the following paragraph.

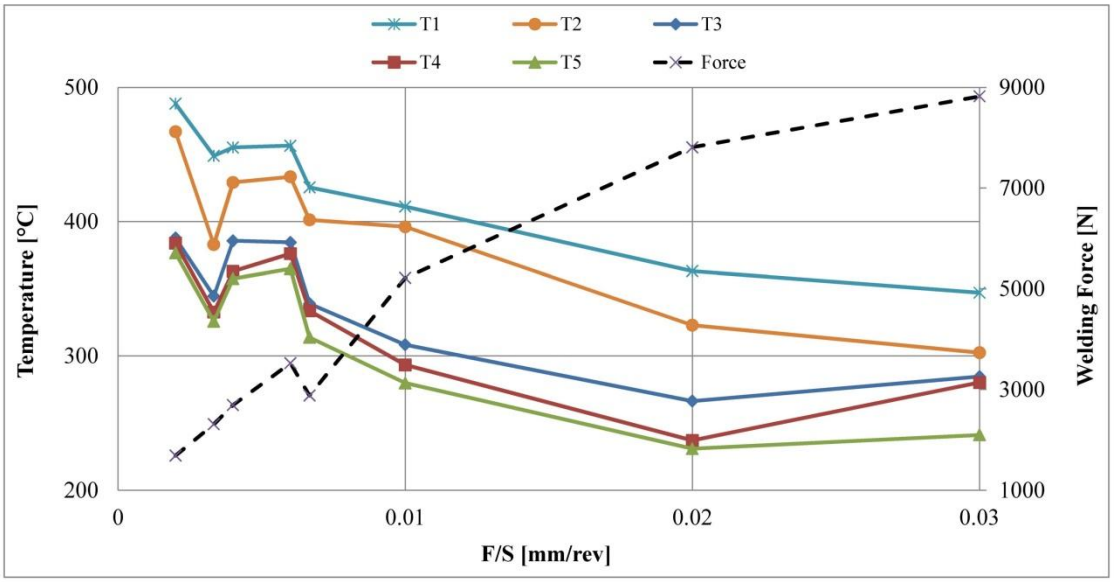

Figure 8 - Welding force and temperature at different position from the welding axis, as a function of the F/S ratio.

3.2 Mechanical characterization

ANOVA (Analysis of Variance) statistical investigation was also carried out on the data coming from the shear test. Table 4 shows the ANOVA output in terms of P-values of the process parameters for shear resistance indicator. Figure 9 shows the main effect plots for shear resistance as a function of the welding parameters. A general good repeatability was found in all cases and all the considered factors (S, F, Z and t) influence the mechanical properties of the joints in terms of

shear resistance, being the p-values very low. Moreover, no significant interaction between the factors can be found except for “S*Z” that has shown a p-value under 0.05. By combining these results with the data coming from the thermal analysis, it is possible to observe that plunging depth and dwell time do not influence the process conditions (temperature and welding force), even if they influence the mechanical properties of the joint.

Table 4. ANOVA output, P-values of the process parameters for shear resistance indicator.

Source	P-value
S	0
F	0.001
Z	0
t	0.001
S*Z	0.001

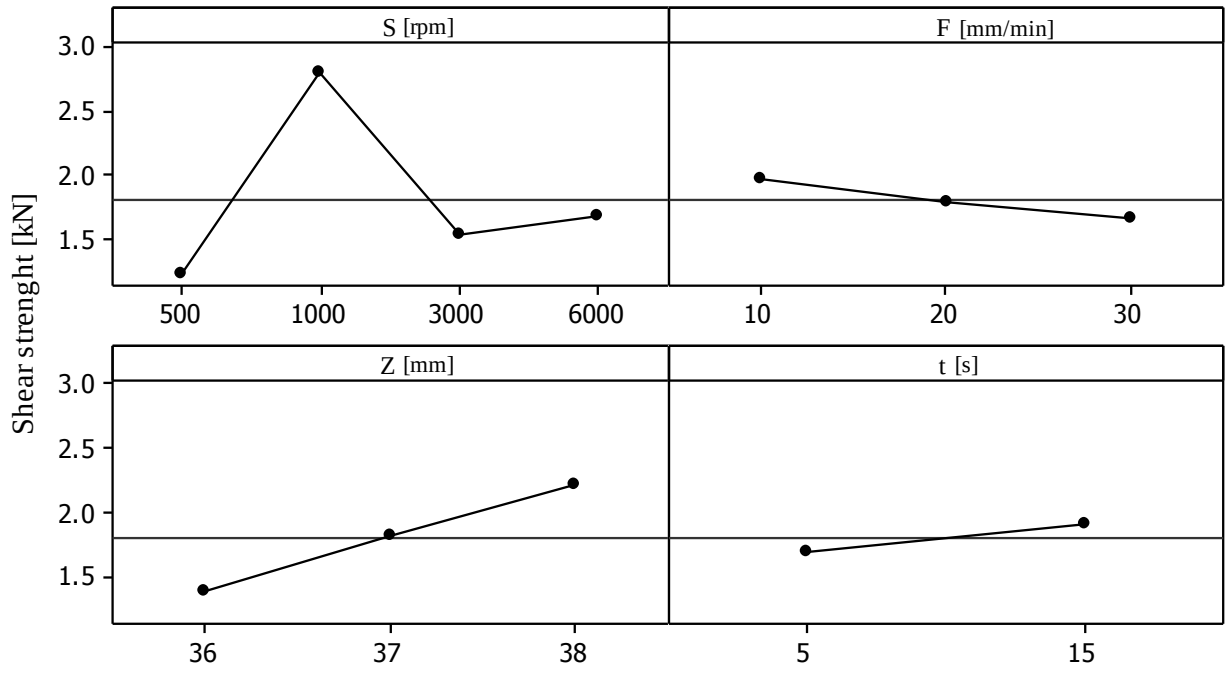

Figure 9 – Main effect plot, data means for shear load at rupture (expressed in kN)

The combined effect of S and F is shown in figure 10a: in this case it is possible to observe how the F parameter has a significant effect only for a limited range of rotational speed while feed rate is effective in the whole tested range. In order to appreciate the effects of the second degree parameter "S*Z", a 3D plot is reported in figure 10b.

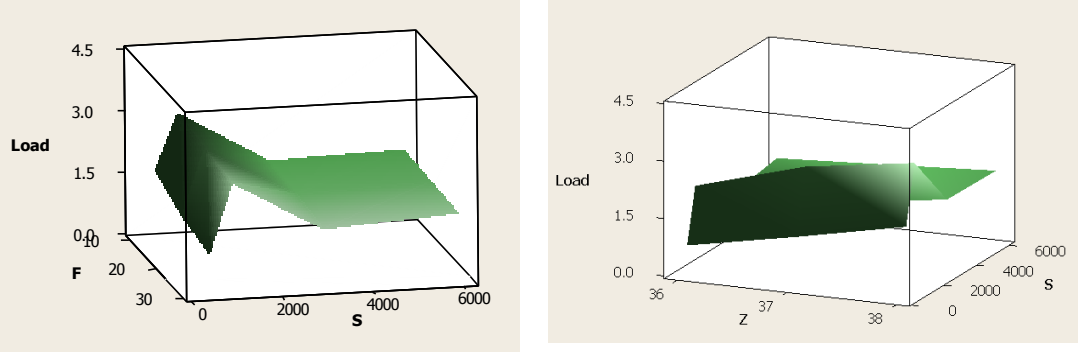

(a) Shear load vs S, F (b) Shear load vs S, Z

Figure 10 - Surface plot, shear load at rupture (expressed in kN) as a function of S,F (a) and as a function of S, Z (b).

As showed in figure 9, the mechanical properties of the joints are strictly related to the rotational speed and in particular an optimal condition (relative maximum of the shear resistance vs. rotational speed curve) was evidenced in correspondence of F=1000 rpm. This is in agreement with some studies reported into the literature [3,18]. Moreover, the increase of feed rate results in a general reduction of mechanical properties. Within the limits of the present investigation, a general increase of the shear resistance can be observed for increasing values of the plunging depth. A similar consideration can be also made for the dwell time.

In order to give more concise information, maximum shear strength, maximum temperatures and maximum welding forces were finally plotted as a function of the feed rate per unit revolution (F/S). Figure 11 shows the shear strength [kN] and the maximum welding temperature [°C] (temperature measured by the thermocouple closest to the welding axis, T1) as a function of F/S ratio [mm/rev]. A power fitting low of the temperature distribution was also plotted together with

the interpolating equation; a very good matching was found ($R^2 = 0.94$). Figure 12 shows the shear strength [kN] and the maximum welding force [N] as a function of F/S ratio [mm/rev] together with a logarithmic fitting equation of the welding force distribution; also in this case a good matching was achieved ($R^2 = 0.94$).

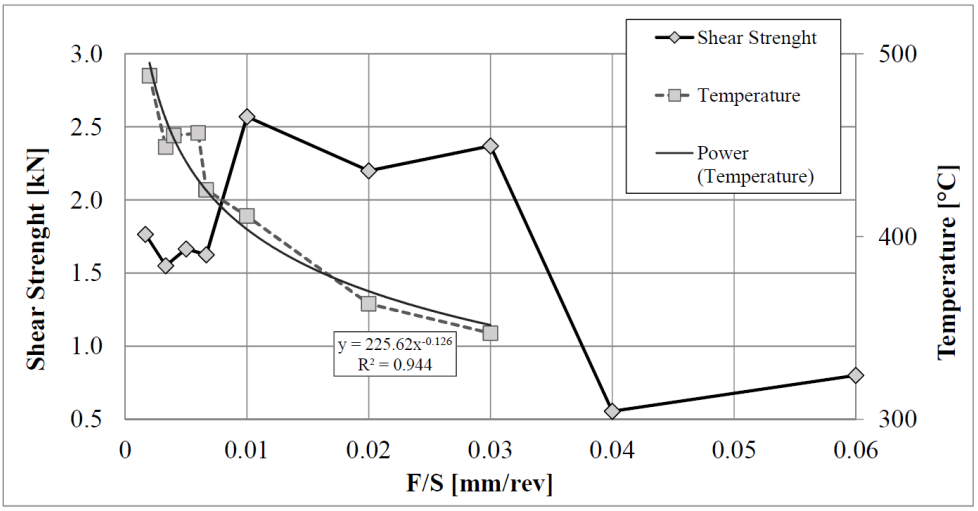

Figure - 11 - Shear strength [kN] and maximum welding temperature [°C] as a function of F/S ratio [mm/rev]; logarithmic fitting of the temperature distribution.

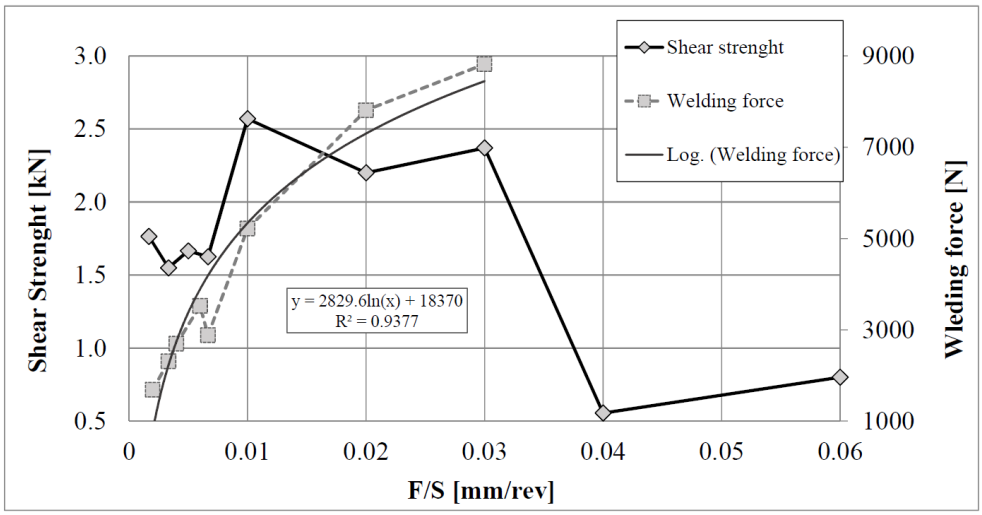

Figure 12 - Shear strength [kN] and maximum welding force [N] as a function of F/S ratio [mm/rev]; logarithmic fitting of the welding force distribution.

The shear strength vs. F/S curve shows an intermediate region in which optimal mechanical properties of the joints can be achieved. For very low values of the F/S ratio the temperature in the joining region is too high, resulting in low welding forces and consequent limited hydrostatic pressure applied to the material. This condition produces joints with limited shear strength. On the opposite, for very high values of the F/S ratio, the temperature of the material is too low and under a certain limit the solid state bonding phenomena does not occur even if a very high pressure, resulting by high axial forces, is applied (see figure 12). Finally, an optimal combination of these two conditions minimizes the thermal effects on the material and, at the same time, increases the compressive (hydrostatic) stress in the joint region.

4. FEM simulation

A 2D model has been developed in DEFORM 2D environment to easily and quickly simulate a FSSW operation in terms of generated heat, temperature distribution and force required. Since it is not possible to simulate the pin rotation using a axisymmetric model, a specific simulation approach has been adopted to compute the heat generated by the pin.

4.1 model description

The approach followed to set up the simulations is based on an analytical model for the heat flux calculus described in [32]. A scheme of the analytical model is reported in figure 13.

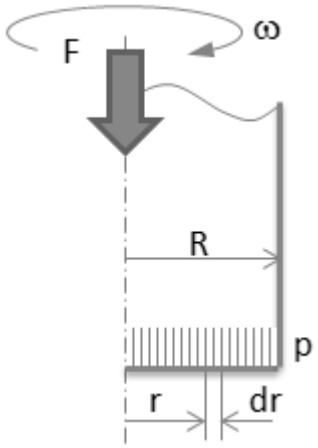

Figure 13 – Scheme of the 2D analytical model.

The heat flux q can be calculated as the product of the torque Mt acting on the pin and due to the friction present at the interface between the pin and the parts to be welded and the angular velocity ω:

$$q = Mt \cdot \omega \tag{2}$$

Where ω is expressed as a function of the rotational speed S:

$$\omega = 2\pi \cdot S/60 \tag{3}$$

While Mt can be calculated as the integral of the infinitesimal torque contribution due to the friction acting at the pin-parts interface:

$$Mt = \int_0^R r \cdot 2\pi \cdot r \cdot p \cdot f \cdot dr = \int_0^R 2\pi \cdot r^2 \cdot p \cdot f \cdot dr \tag{4}$$

Where R is the pin radius, p is the pressure in r and f is the friction coefficient.

If p is considered uniformly distributed, it can be calculated as:

$$p = F \diagup A \tag{5}$$

Where F is the vertical force acting on the pin and A the contact area of the pin; afterwords, Mt can be calculated as:

$$Mt = \frac{2}{3}\pi \cdot R^3 \cdot p \cdot f \tag{6}$$

When these equations were implemented in the 2D FEM model, the integral was transformed in a sum of finite terms. Moreover, since the FEM engine can calculate the local pressure acting on the single boundary element of the pin mesh, the pressure can be defined as a function of the radial position and Mt can be more correctly expressed as:

$$Mt = \sum_{i=1}^{n-1} 2\pi \cdot r_{i,i+1}^2 \cdot \left(r_{i+1} - r_i\right) \cdot p_{i,i+1} \cdot f \tag{7}$$

Where n is the total number of the pin boundary nodes at the interface between pin and parts, r_i and r_{i+1} are the radius values of the i-th and (i+1)-th nodes, $r_{i,i+1}$ is the average value of these two radii and $p_{i,i+1}$ is the pressure acting on the boundary element included between the i-th and (i+1)-th nodes (see figure 14).

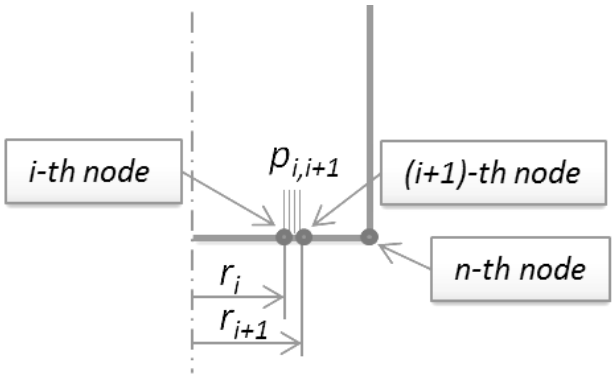

Figure 14 – Scheme of the 2D FEM model.

Then, the heat flux generated at the pin-workpiece interface along the element defined by the i-th and the (i+1)-th nodes corresponds to the single term of the last expression multiplied by the angular velocity ω and divided by the circular area, defined by the same nodes. This heat flux was imposed to the pin as boundary condition. Thanks to the coupled thermo-mechanical simulation set up, the imposed heat flux locally increases the temperature of both the pin and the welding region as the tool rotates. Since the set of calculus previously described cannot be carried out directly into the model, an external routine was developed for this purpose.

4.2 model validation

Some simulations were finally run, the process parameters were set according to the experimental tests, while material properties were selected from Deform database. Figure 15 shows an example of the simulative temperature distribution generated by the following process parameters: S= 5000 rpm, F= 10 mm/min, Z= 3.7 mm, t= 1 s.

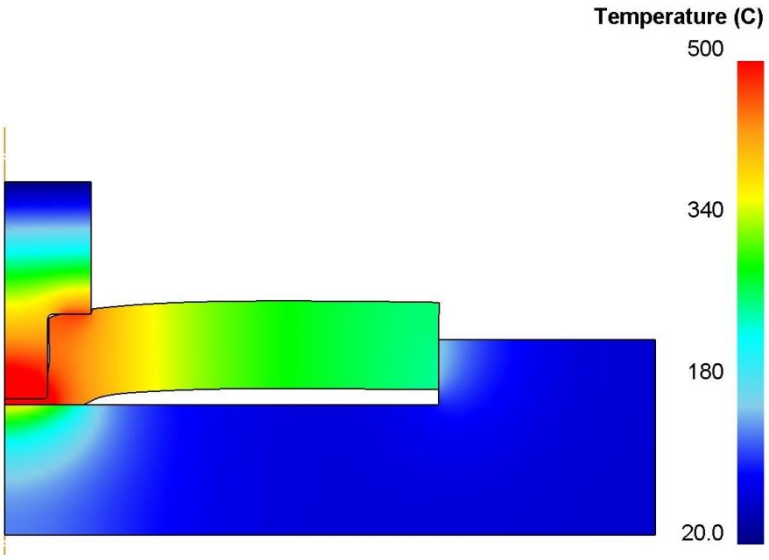

Figure 15 – Example of FEM output: temperature distribution (S = 5000 rpm, F = 10 mm/min, Z = 3.7 mm).

A validation of the FEM model was performed through the comparison of numerical and experimental data. Figures 16 a-c-e show a comparison between numerical and experimental results in terms of temperature distribution at 4 mm from the joint axis vs. axial stroke curves (S=1000 rpm and F=30 mm/min, S=3000 rpm and F=20 mm/min, S=5000 rpm and F=10 mm/min). The same kind of comparison was executed in terms of maximum axial force and reported in figures 16 b-d-f. If we consider the complexity of the simulated process, a satisfactory matching was achieved: the simulative curves well approximate the corresponding experimental ones and the maximum estimated values differ at least for 17% in forces and 1,6% in temperatures. An acceptable matching was achieved in terms of curves behaviour. It must be noted that a significant discrepancy was only observed for the welding forces in the condition S=1000 rpm and F=30 mm/min; in this specific case, having a very low F/S ratio, the FEM model is not able to predict a particular behaviour (different from all the other conditions) evidenced by the experiments.

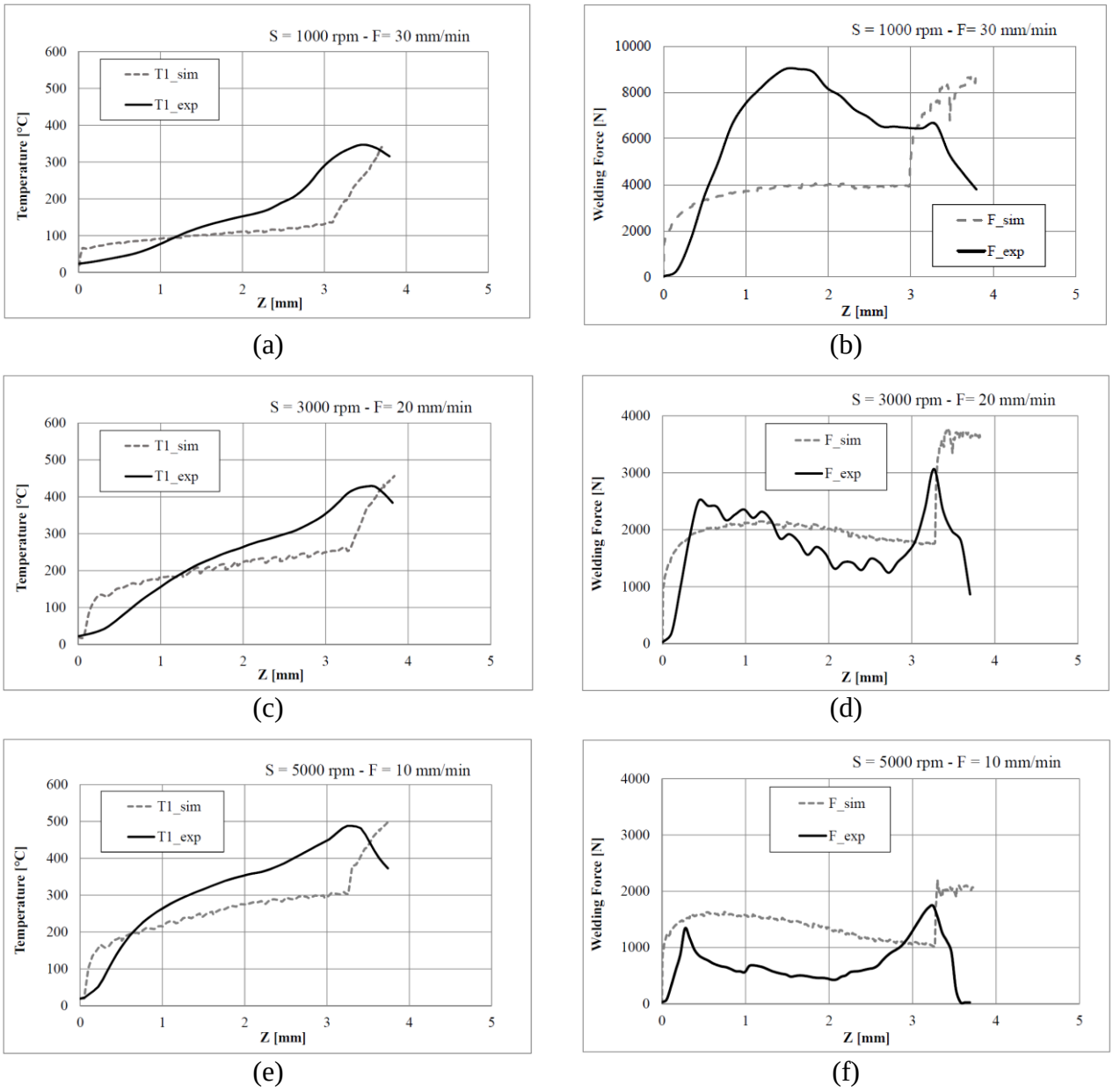

Figure 16 - Comparison between numerical and experimental results in terms of temperature distribution at 4 mm from the joint axis vs. axial stroke curves (a-c-e) and maximum axial force vs. axial stroke (b-d-f).

Basing on the previous considerations, the mean (hydrostatic) stress and the temperature in the welding region are strictly related to the joint shear strength. Then, a simulative predictive index of the joint resistance was defined basing on these two parameters and reported in eq. 8.

$$Resistance\ index = \frac{|\sigma_{idr}|T^2}{k} \quad (8)$$

Where k is a constant value (in this specific case set equal to 30000), σ_{idr} is the mean stress and T the maximum temperature measured in the welding region at the last simulative step. A comparison between experimental and simulative results in terms of shear strength and predictive resistance index as a function of the F/S ratio is reported in figure 17. A good matching between experimental and simulative curves was achieved. A significant discrepancy can be observed only in the first part of the curve, were the combination of very high tool rotational speed and low feed rate result in severe thermal conditions and low welding forces.

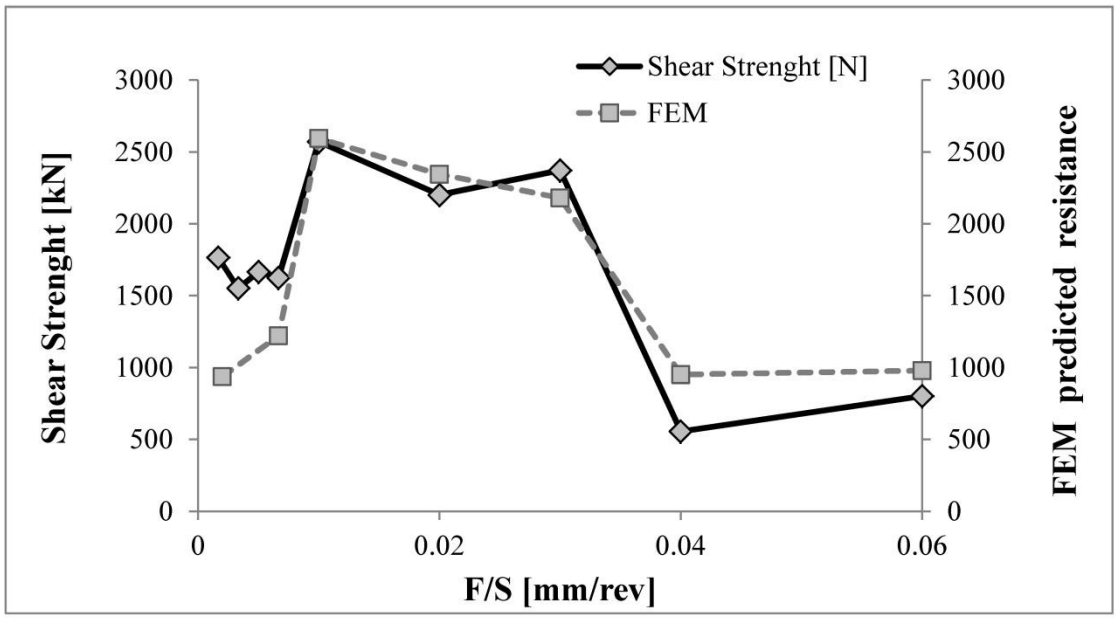

Figure 17 - Comparison between simulative and experimental results in terms of shear strength and predictive resistance index as a function of the F/S ratio.

5. Conclusions

An experimental campaign was carried out to study how the FSSW process parameters affect the thermal distribution in the welding region, the welding forces and the mechanical properties of the

joints. A dependency of welding forces and maximum achieved temperature on rotational speed and feed rate was observed: high values of rotational speed and low values of feed rate lead to lower welding forces and higher welding temperatures. The mechanical properties of the joints are strictly related to these aspects. In particular, the shear resistance of the joints reaches an optimum for intermediate conditions of temperature and welding forces, when the material temperature and pressure are high enough for the solid state phenomena occurrence. Moreover, an increase of the shear resistance can be observed for increasing values of plunging depth and dwell time.

A simulative model for the evaluation of thermo-mechanical effects in FSSW was proposed in this study. The peculiarity of the FEM model set up for this work is a 2D approach used for the simulation of a 3D problem. This solution resulted in a very rapid simulative tool, if compared with 3D FSSW simulations that usually require several hours or even days for the computation. An index for the prediction of the joint shear resistance using FEM simulations was finally proposed and validated.

References

[1] Thomas WM, Nichola ED, Needam JC, Murch MG, Templesmith P, Dawes CJ. 1991, GB Patent Application No. 9125978-8.

[2] Thomas WM, Nichola ED, Needam JC, Murch MG, Templesmith P, Dawes CJ. 1995, US Patent Application No. 5460317.P.L.

[3] Sakano R, Murakami K, Yamashita K, Hyoe T, Fuzimoto M, Inuzuka M et al. Development of spot FSW robot system for automotive body members. In: Proceedings of the 3rd international symposium of friction stir welding, Kobe, Japan, September 27–28, 2001.

[4] Iwashita T. Method and apparatus for joining. US patent, 6601751 B2; August 5, 2003.

[5] Lathabai S, Painter, MJ, Cantin GMD, Tyagi VK. Friction spot joining of an extruded Al–Mg–Si alloy. Scripta Mater. 2006;55:899–902.

[6] Yuana W, Mishraa RS, Webba S, Chenb YL, Carlsonb B, Herlingc DR, Grantc GJ. Effect of tool design and process parameters on properties of Al alloy 6016 friction stir spot welds. Journal of Materials Processing Technology 2011;211:972–977.

[7] Hirasawaa S, Badarinarayanb H, Okamotoc K, Tomimurad T, Kawanamia T. Analysis of effect of tool geometry on plastic flow during friction stir spot welding using particle method. Journal of Materials Processing Technology 2010;210:1455–1463.

[8] Shi SG, Westgate SA. Resistance spot welding of high-strength steel sheet. Corporate research program report, The Welding Institute (TWI) 2003;767.

[9] Spinella DJ, Brockenbrough JR, Fridy JM. Trend in aluminum resistance spot welding for the automotive industry. Weld J. 2005;84(1):34–40.

[10] Dashatan SH, Azdast T, Ahmadi S, Bagheri A. Friction stir spot welding of dissimilar polymethyl methacrylate and acrylonitrile butadiene styrene sheets. Materials and Design 2013;45:135–141.

[11] Bilici MK, Yükler AI. Influence of tool geometry and process parameters on macrostructure and static strength in friction stir spot welded polyethylene sheets. Materials and Design 2012;33:145–152.

[12] Fanelli P, Vivio F, Vullo V. Experimental and numerical characterization of Friction Stir Spot Welded joints. Engineering Fracture Mechanics 2012;81:17–25.

[13] Jata KV, Semiatin SL. Continuous dynamic recrystallization during friction stir welding of high strength aluminum alloys. Scripta Mater 2000;43:743–9.

[14] Matsumoto K, Sasabe S. Lap joints of aluminium alloys by friction stir welding. In: Proc. 3rd Int. Symp. FSW, Kobe, Japan; 2001.

[15] Badarinarayan H, Shi Y, Li X, Okamoto K. Effect of tool geometry on hook formation and static strength of friction stir spot welded aluminum 5754-O sheets. Int. J. Mach. Tools Manuf. 2009;49(11):814–823.

[16] Badarinarayan H, Yang Q, Zhu S. Effect of tool geometry on static strength of friction stir spot-welded aluminum alloy. Int. J. Mach. Tools Manuf. 2009;49(2):142–148.

[17] Jonckheere C, de Meester B, Cassiers C, Delhaye M, Simar A. Fracture and mechanical properties of friction stir spot welds in 6063-T6 aluminum alloy. Int. J. Adv. Manuf. Technol. 2012;62:569–575.

[18] Arul SG, Miller SF, Kruger GH, Pan TY, Mallick PK, Shih AJ. Experimental study of joint performance in spot friction welding of 6111-T4 aluminum alloy. Sci. Technol. Weld. Join 2008;13:629–637.

[19] Freeney T, Sharma SR, Mishra RS. Effect of Welding Parameters on Properties of 5052 Al Friction Stir Spot Welds. SAE Technical Series 2006;01-0969.

[20] Tozaki Y, Uematsu Y, Tokaji K. Effect of processing parameters on static strength of dissimilar friction stir spot welds between different aluminium alloys. Fatigue Fract. Eng. Mater. 2007;30:143–148.

[21] Merzoug M, Mazari M, Berrahal L, Imad A. Parametric studies of the process of friction spot stir welding of aluminium 6060-T5 alloys. Mater Des 2010;31(6):3023–3028.

[22] Yin YH, Sun N, North TH, Hu SS. Hook formation and mechanical properties in AZ31 friction stir spot welds. J. Mater. Process. Technol. 2010;210(14):2062–2070.

[23] Bozzi S, Helbert-Etter AL, Baudin T, Klosek V, Kerbiguet JG, Criquid B. Influence of FSSW parameters on fracture mechanisms of 5182 aluminium welds. J. Mater. Process. Technol. 2010;210(11):1429–1435.

[24] Gerlich A, Su P, Bendzsak GJ, North TH. Numerical modeling of FSW spot welding: preliminary results. Friction Stir Welding and Processing III, TMS 2005.

[25] Langerman M, Kvalvik E. Modeling plasticised aluminum flow and temperature fields during friction stir welding. In: Proceedings of the 6th ASME–JSME Thermal Engineering Joint Conference, TED-AJ03-133 2003.

[26] Colegrove PA, Shercliff HR. Modeling the friction stir welding of aerospace alloys. In: Proceedings of the 5th International FSW Symposium 2004.

[27] Mandal S, Rice J, Elmustafa AA. Experimental and numerical investigation of the plunge stage in friction stir welding. J. Mater. Process Technol. 2008;203:411–9.

[28] Awang M, Mucino VH, Feng Z, David SA. Thermo-mechanical modeling of friction stir spot welding (FSSW) process: use of an explicit adaptive meshing scheme. SAE Int 2005;01:1251.

[29] Rajamanickam N, Balusamy V, Madhusudhann RG, Natarajan K. Effect of process parameters on thermal history and mechanical properties of friction stir welds. Materials and Design 2009;30(7): 2726–2731.

[30] Zhang Z, Zhang HW. Numerical studies on controlling of process parameters in friction stir welding. Journal of Materials Processing Technology 2008;209:241–270.

[31] D'Urso G, Longo M, Giardini C. Friction Stir Spot Welding (FSSW) of Aluminum sheets: Experimental and Simulative Analysis. Key Engineering Materials 2013;549:477-483.

[32] Frigaard O, Grong O, Midling OT. A Process Model for Friction Stir Welding of age hardening aluminum alloys. Metallurgical and Materials Transactions A, 2001;32A:1189-1200.

Short biography of the author

Gianluca D'Urso is Assistant Professor at the Department of Engineering at University of Bergamo, Deputy Director of GITT - Centre on Innovation Management and Technology Transfer. Degree in Management Engineering at the University of Bergamo (Italy). Ph.D. in Manufacturing Engineering at the University of Padova (Italy). Member of AITEM, the Italian Association of Manufacturing Engineers. His main research activities include analysis of joining technologies based on FSW (Friction Stir Welding) by means of experimental and simulative (FEM) methods, experimental and FEM analysis of forming and machining processes, micro-fabrication technologies using micro-EDM (Electro Discharge Machining) and EBL (Electron Beam Lithography).

Figure_01
Click here to download high resolution image

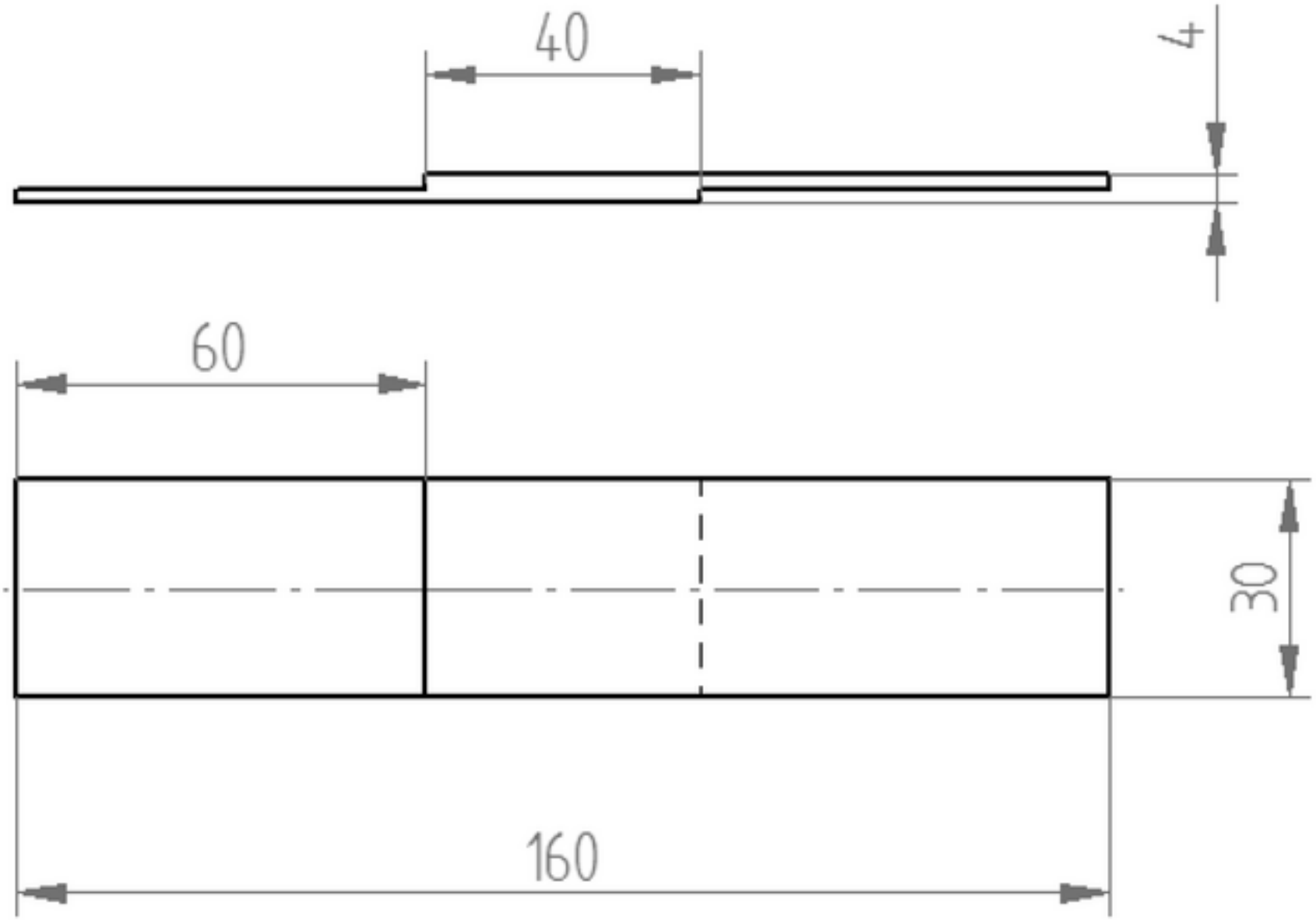

Figure_02
Click here to download high resolution image

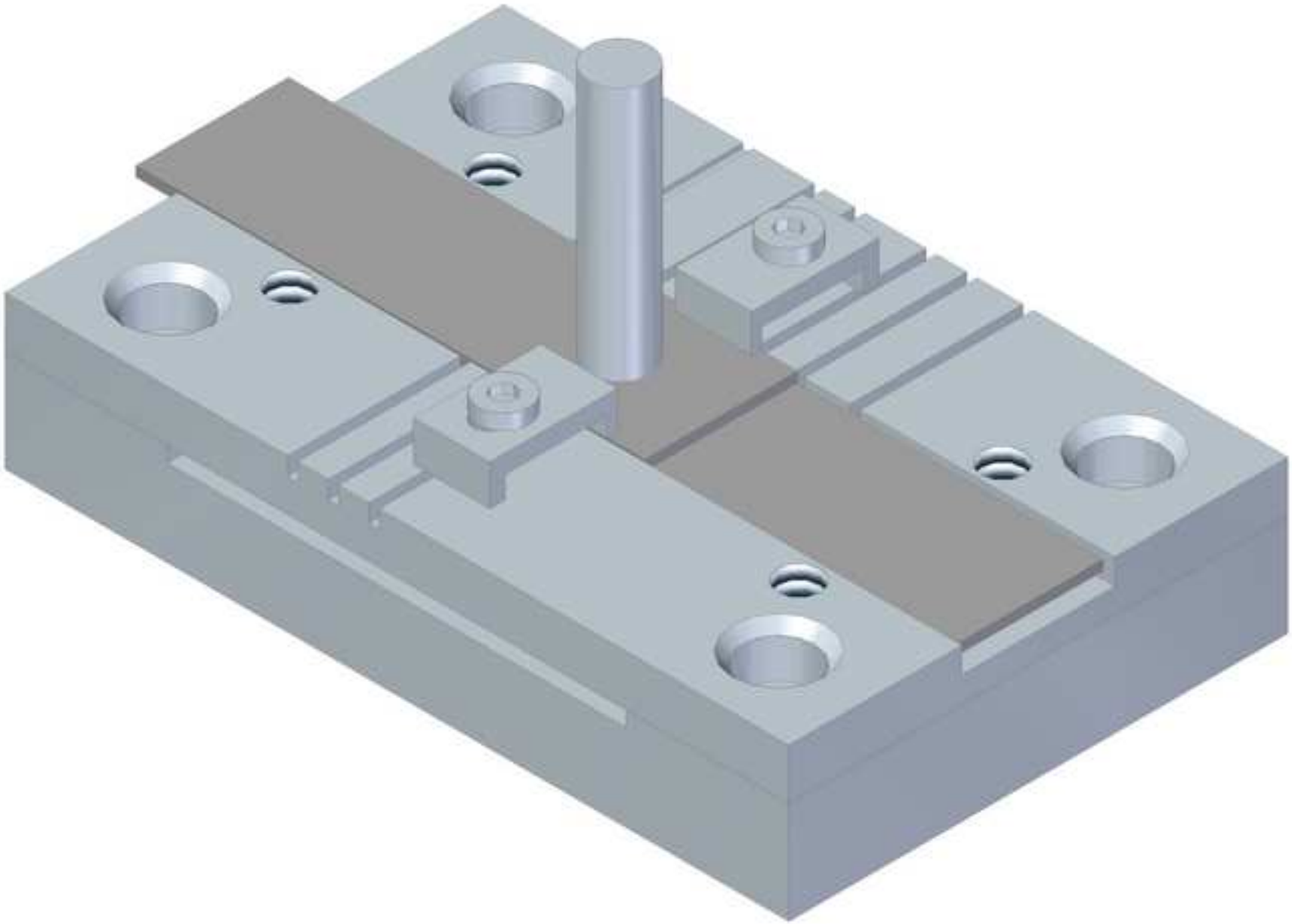

Figure_03
Click here to download high resolution image

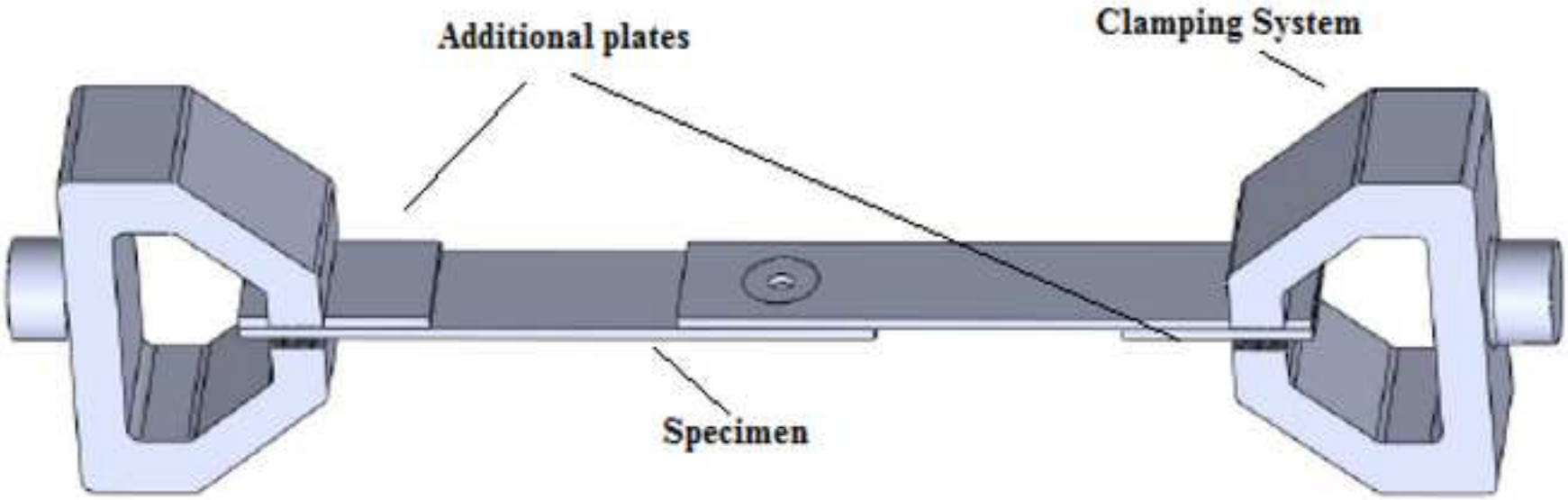

Figure_04a

Click here to download high resolution image

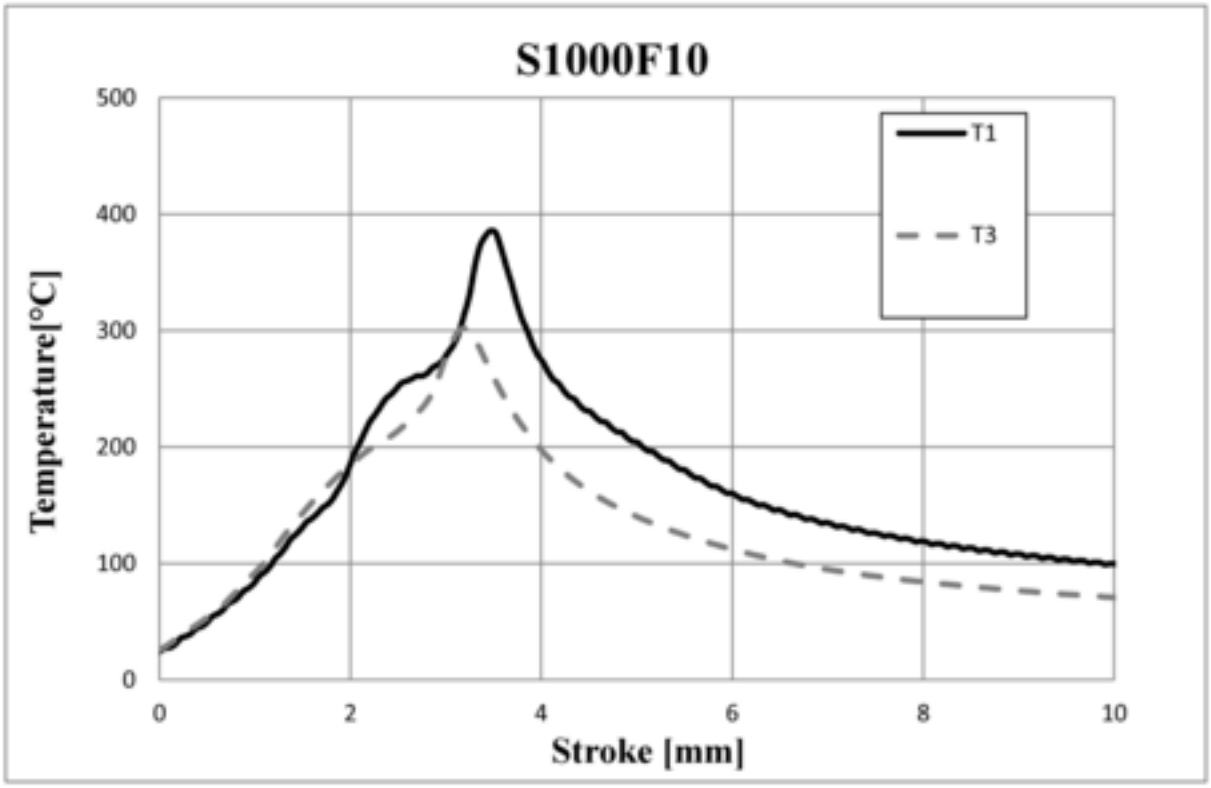

Figure_04b

Click here to download high resolution image

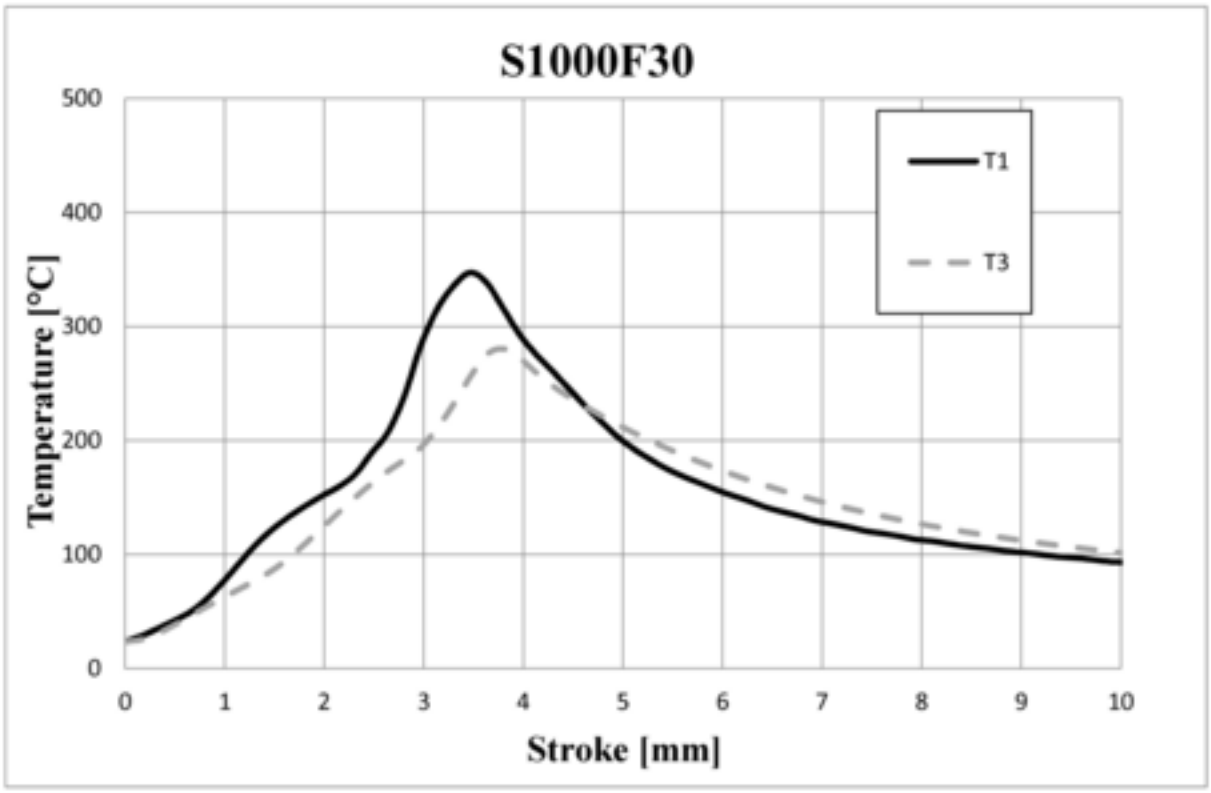

Figure_04c

Click here to download high resolution image

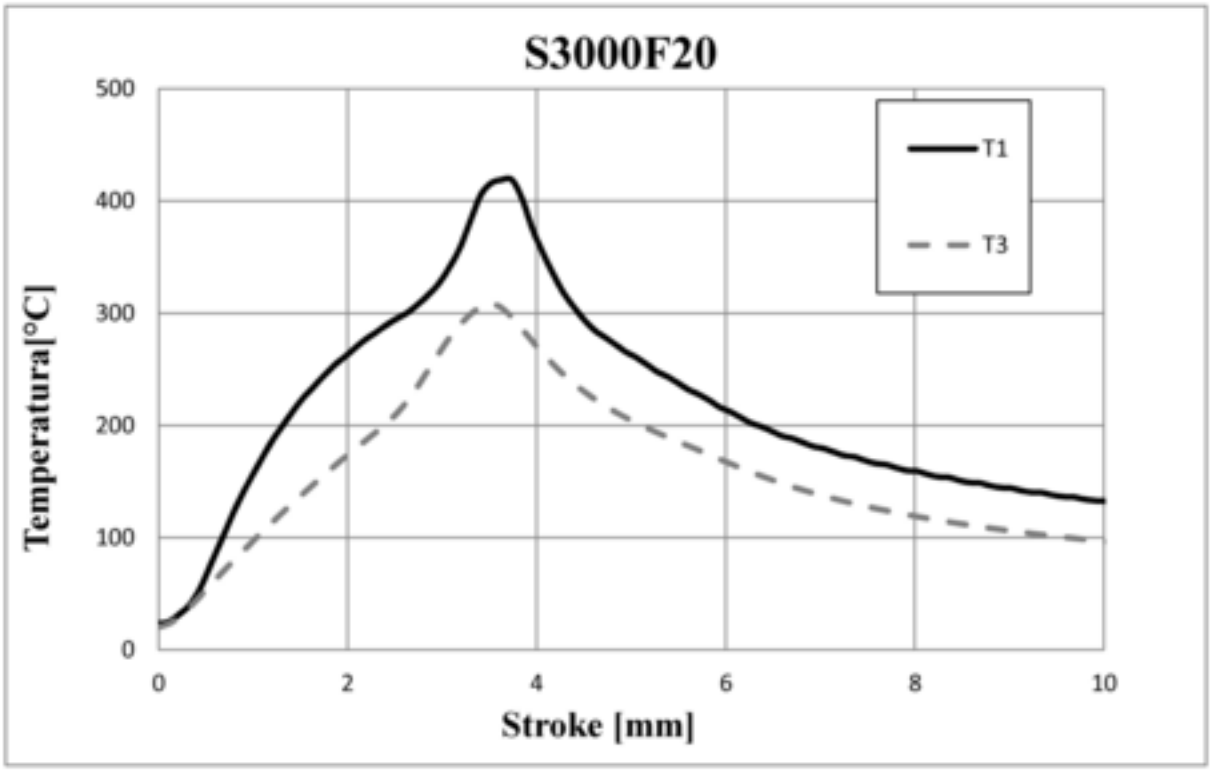

Figure_04d
Click here to download high resolution image

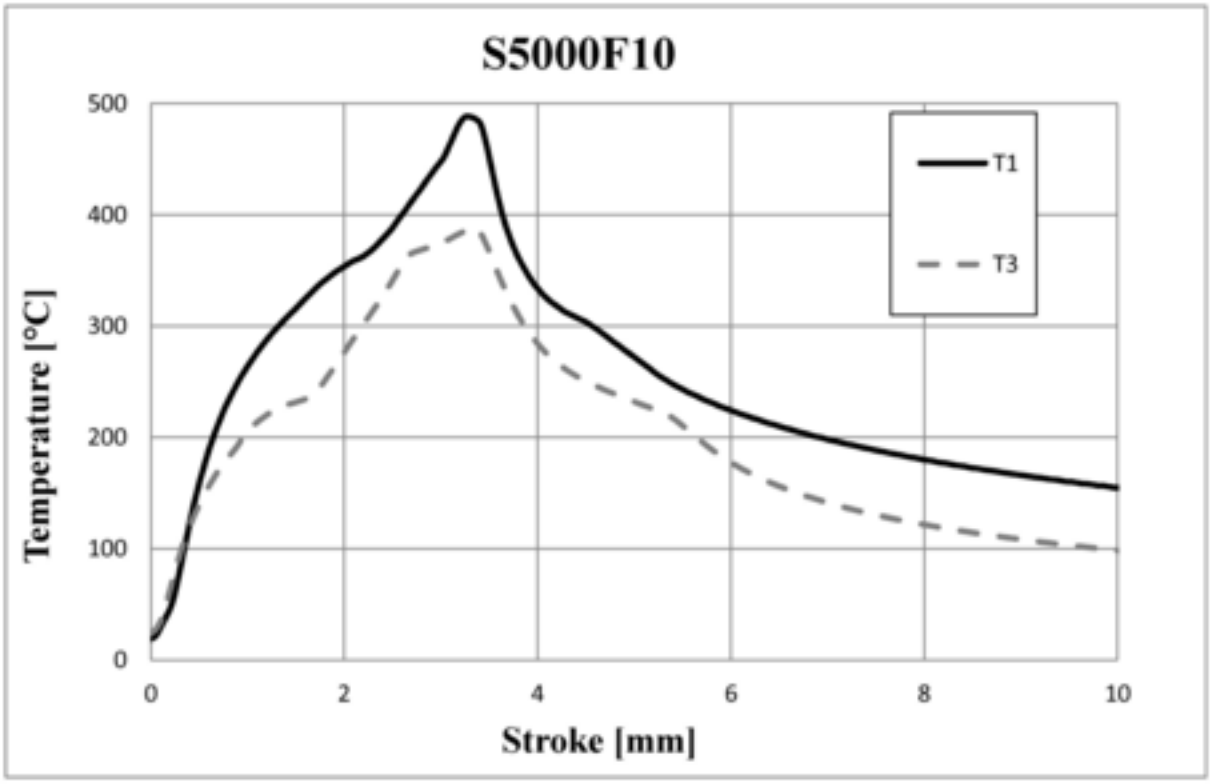

Figure_04e

Click here to download high resolution image

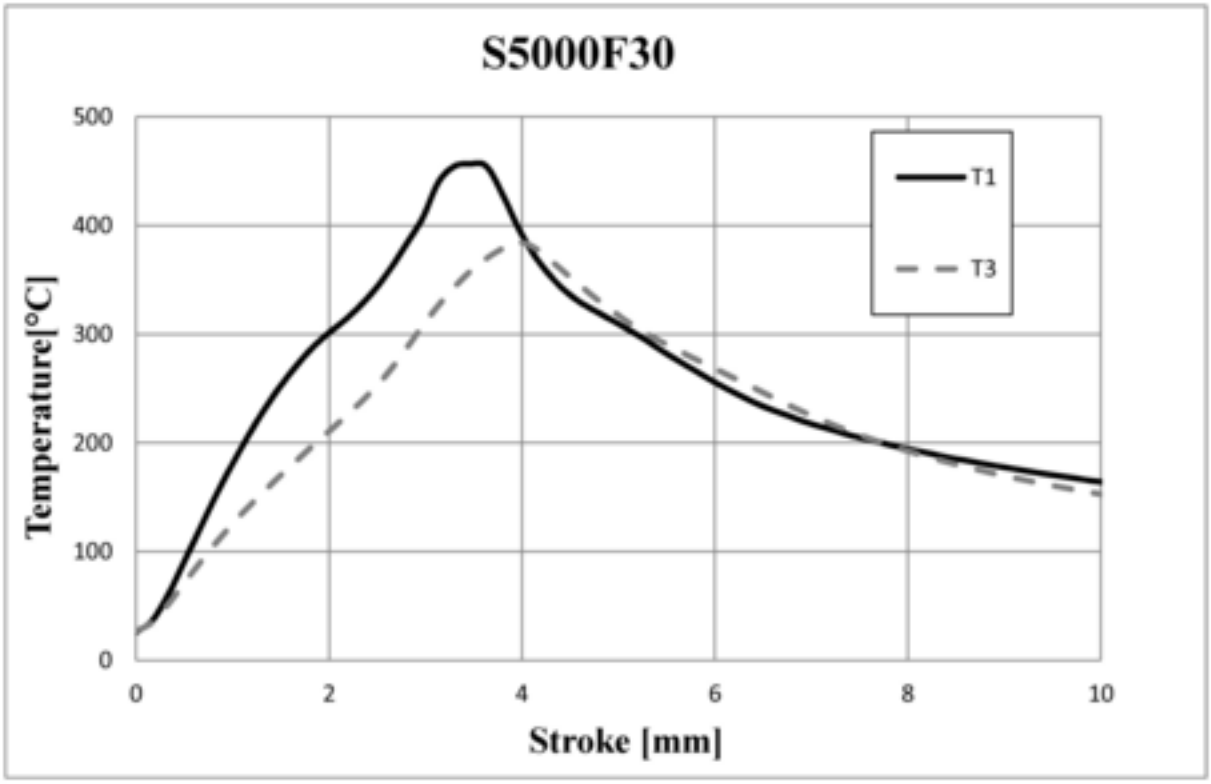

Figure_05
Click here to download high resolution image

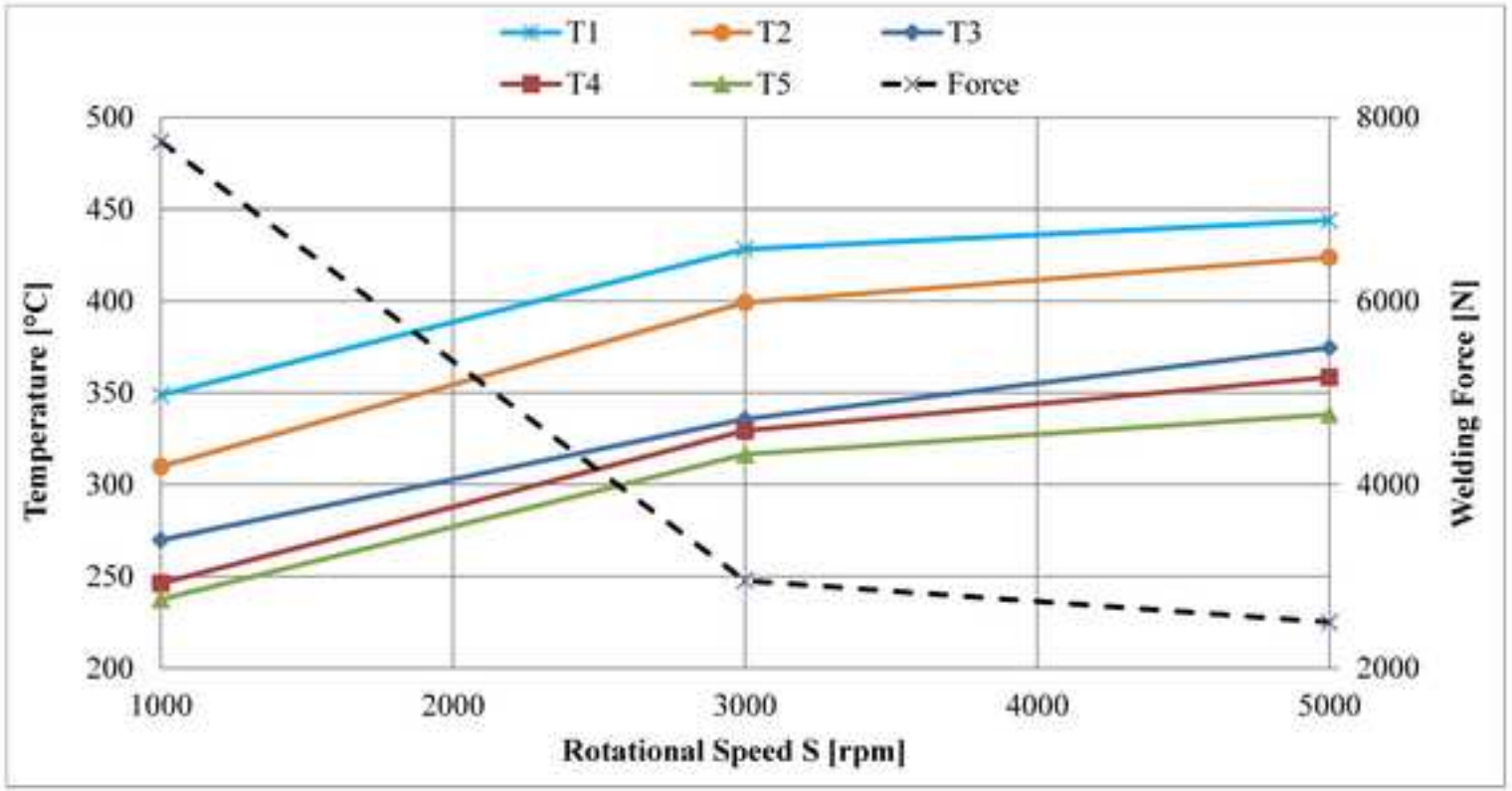

Figure_06
Click here to download high resolution image

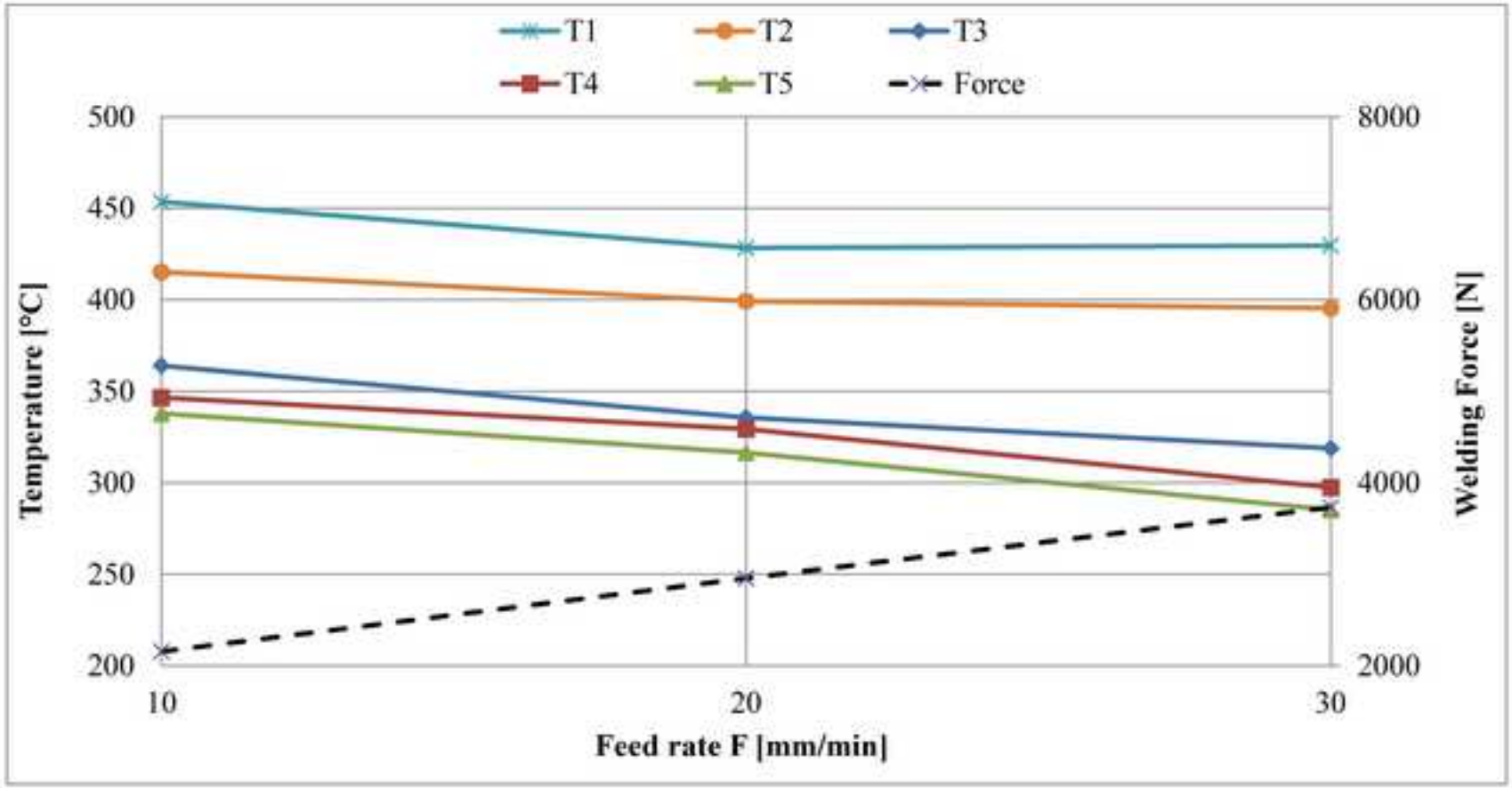

Figure_07
Click here to download high resolution image

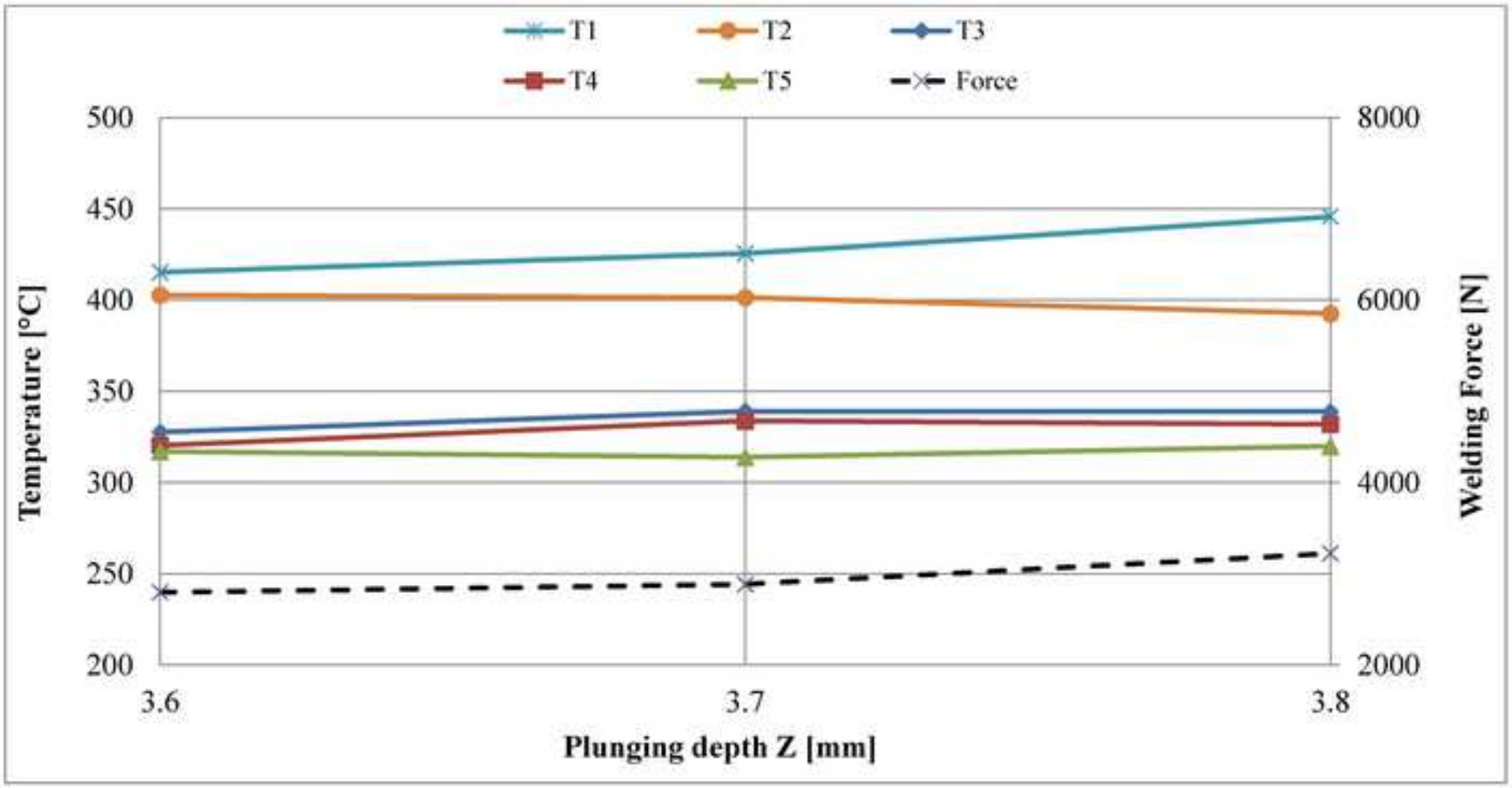

Figure_08
Click here to download high resolution image

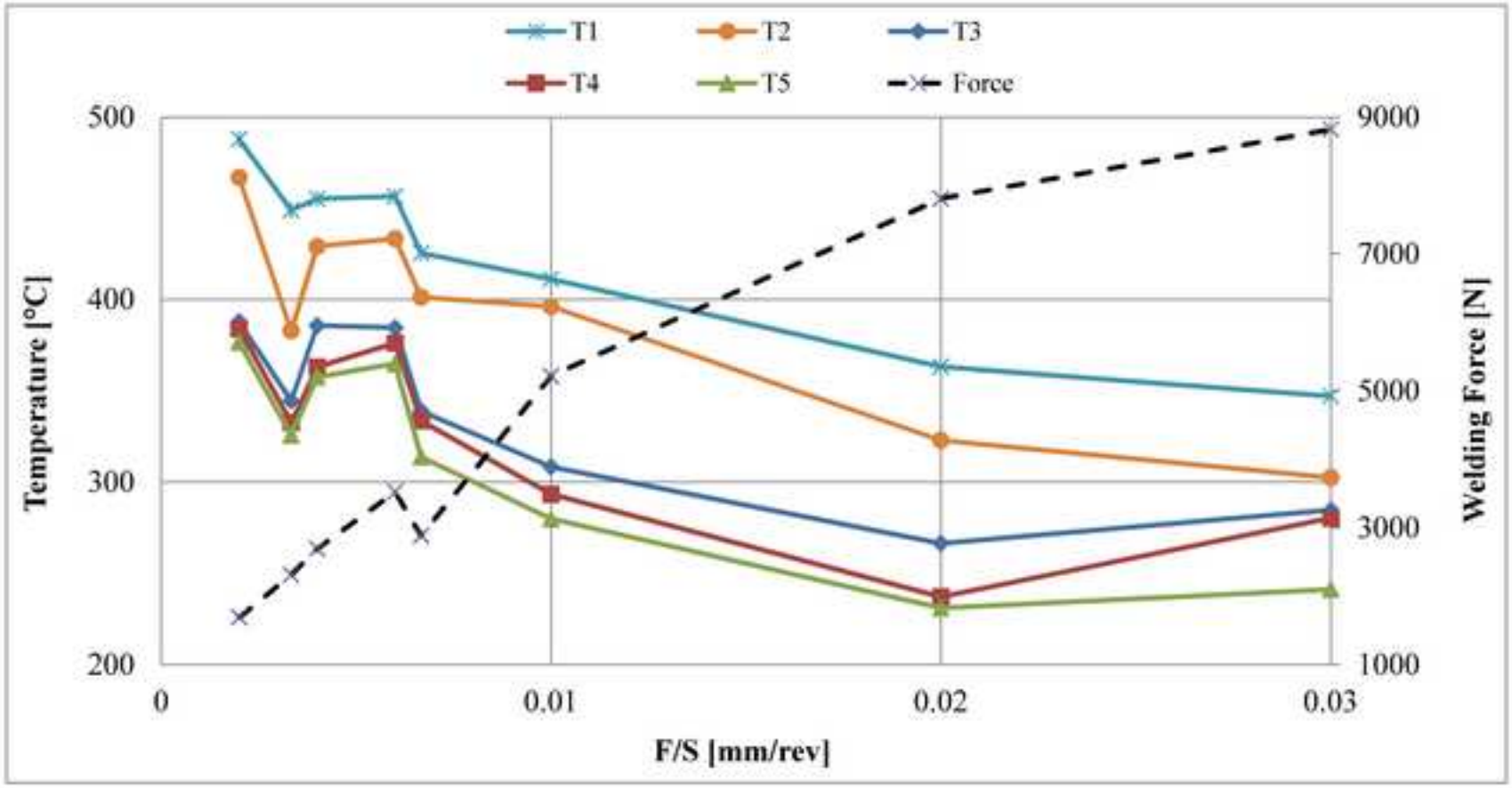

Figure_09

Click here to download high resolution image

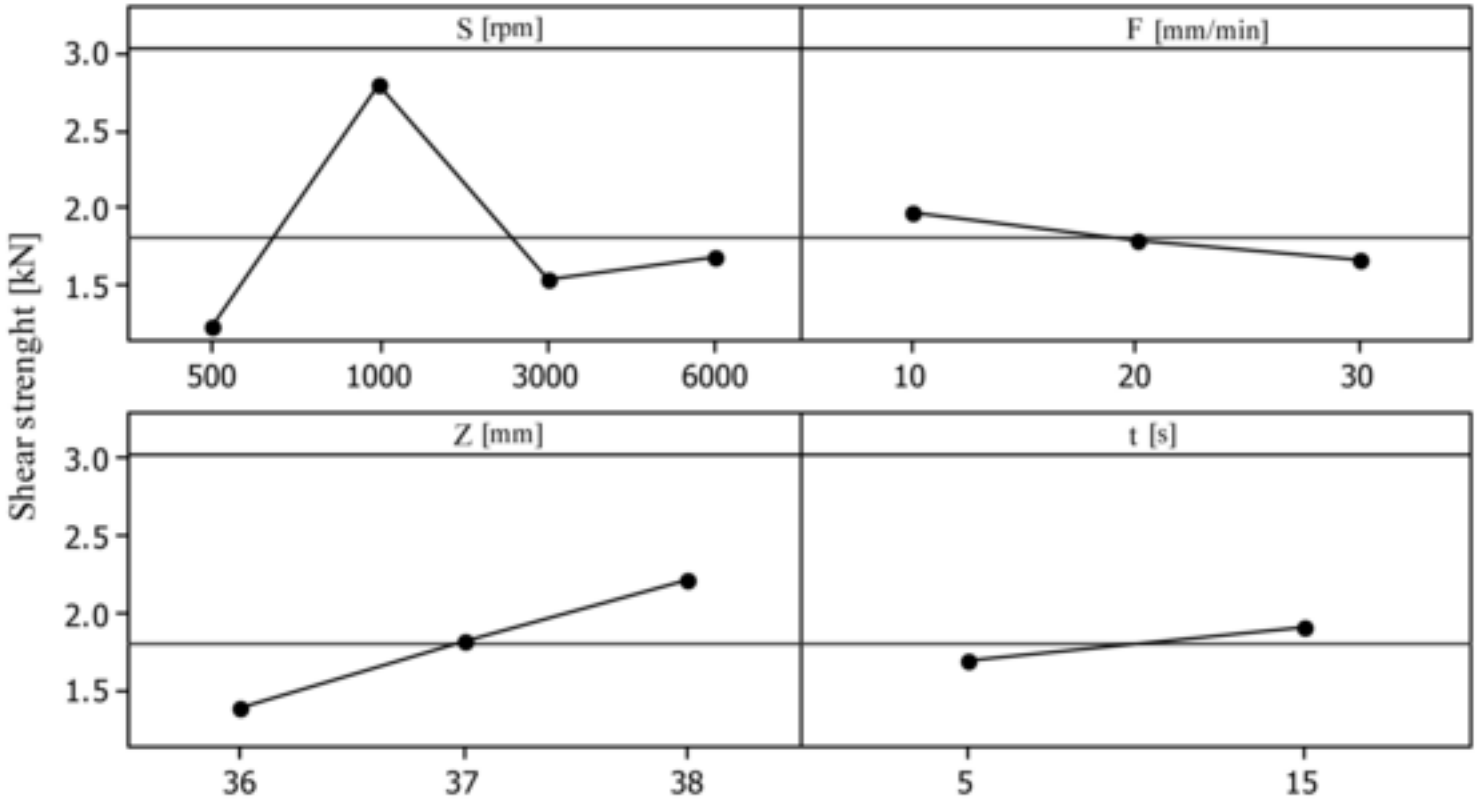

Figure_10a
Click here to download high resolution image

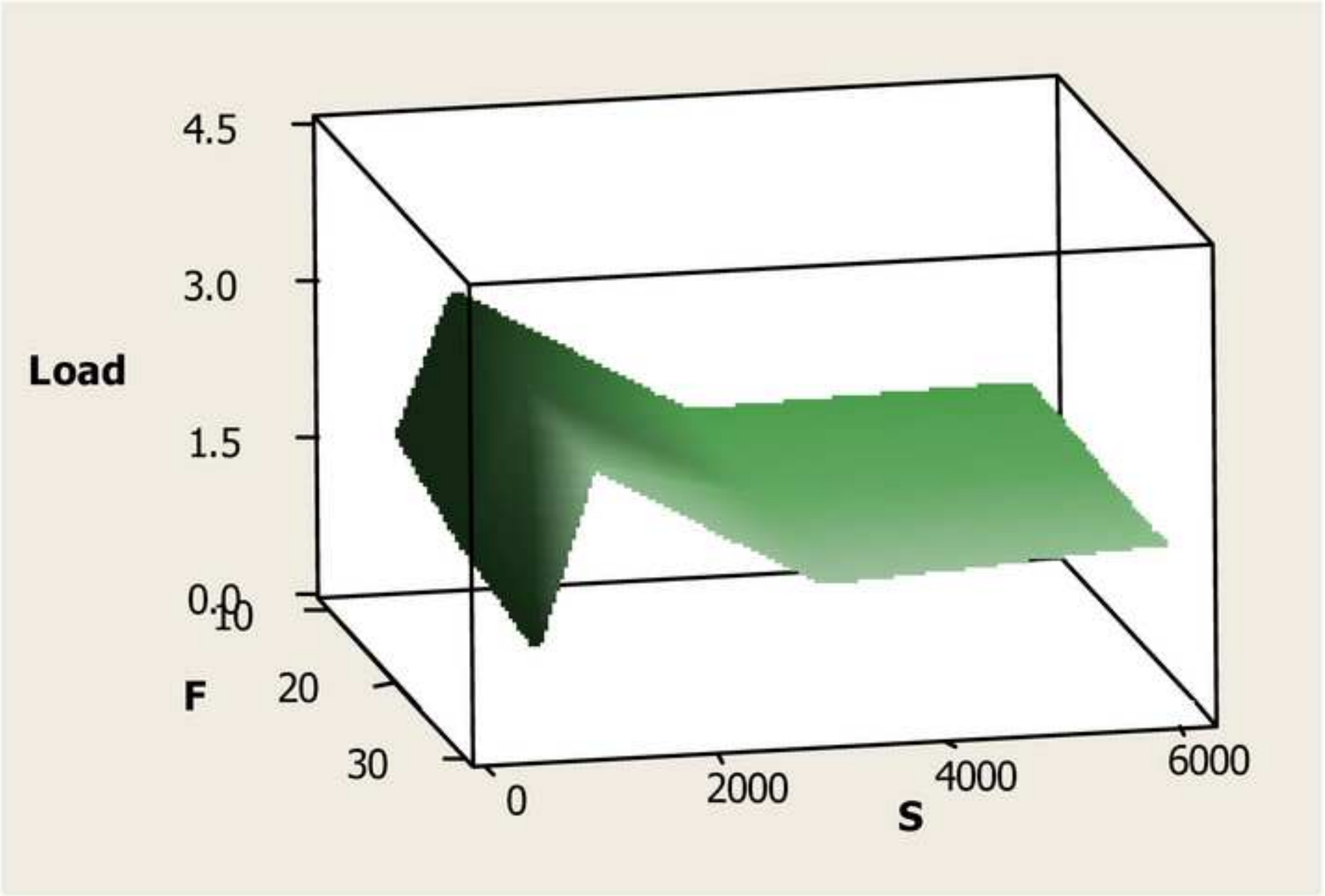

Figure_10b

Click here to download high resolution image

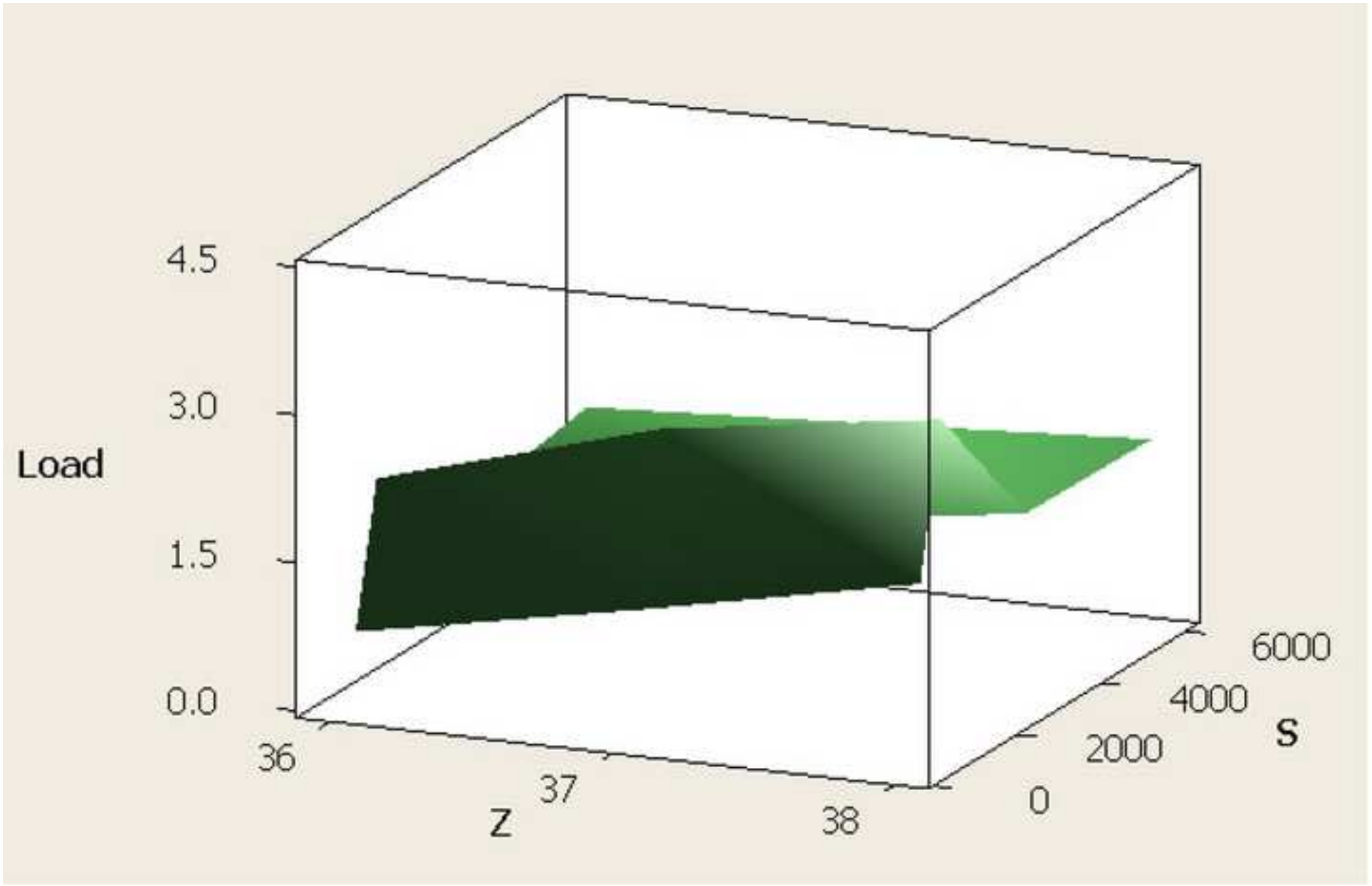

Figure_11
Click here to download high resolution image

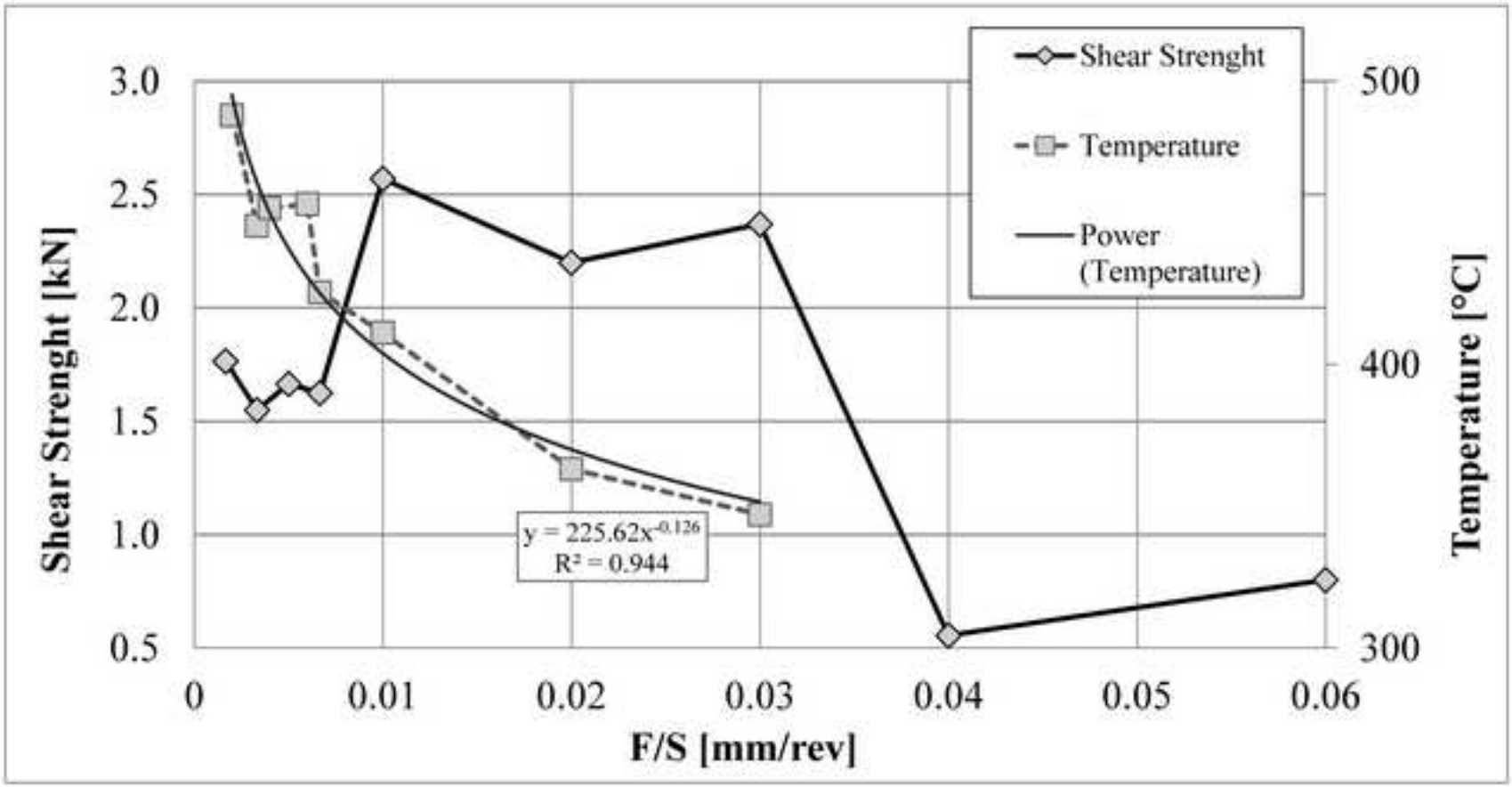

Figure_12
Click here to download high resolution image

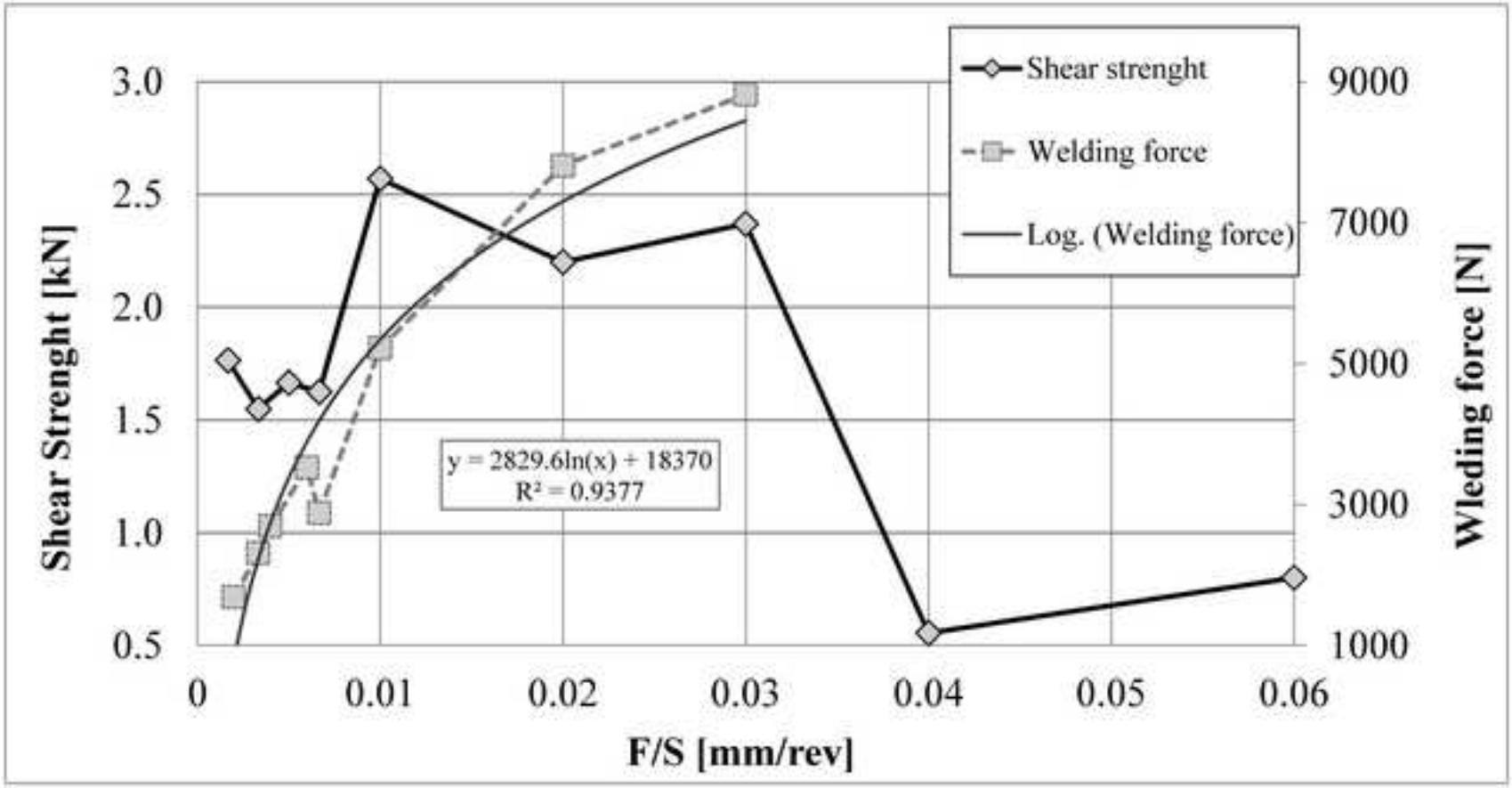

Figure_13
Click here to download high resolution image

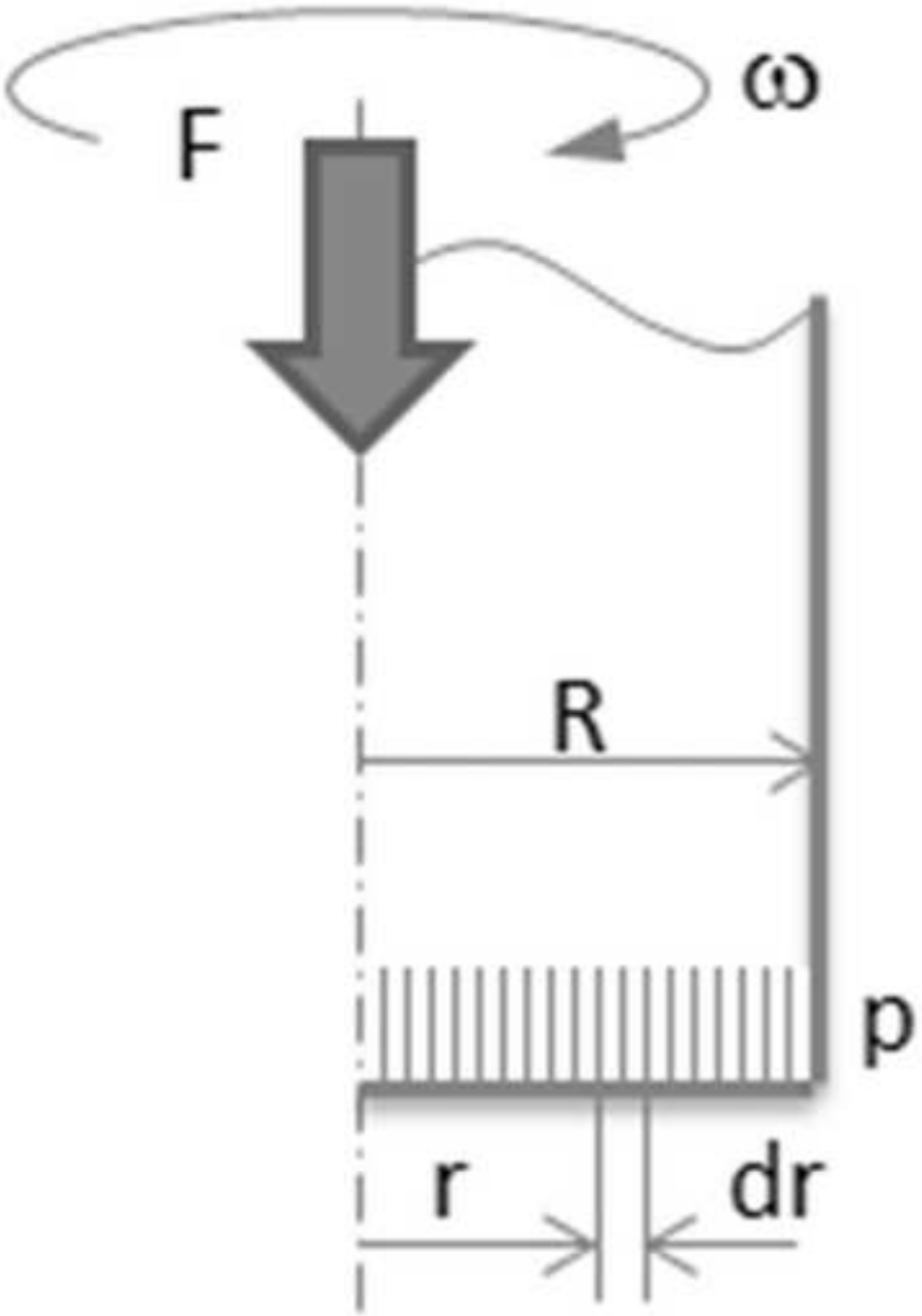

Figure_14
Click here to download high resolution image

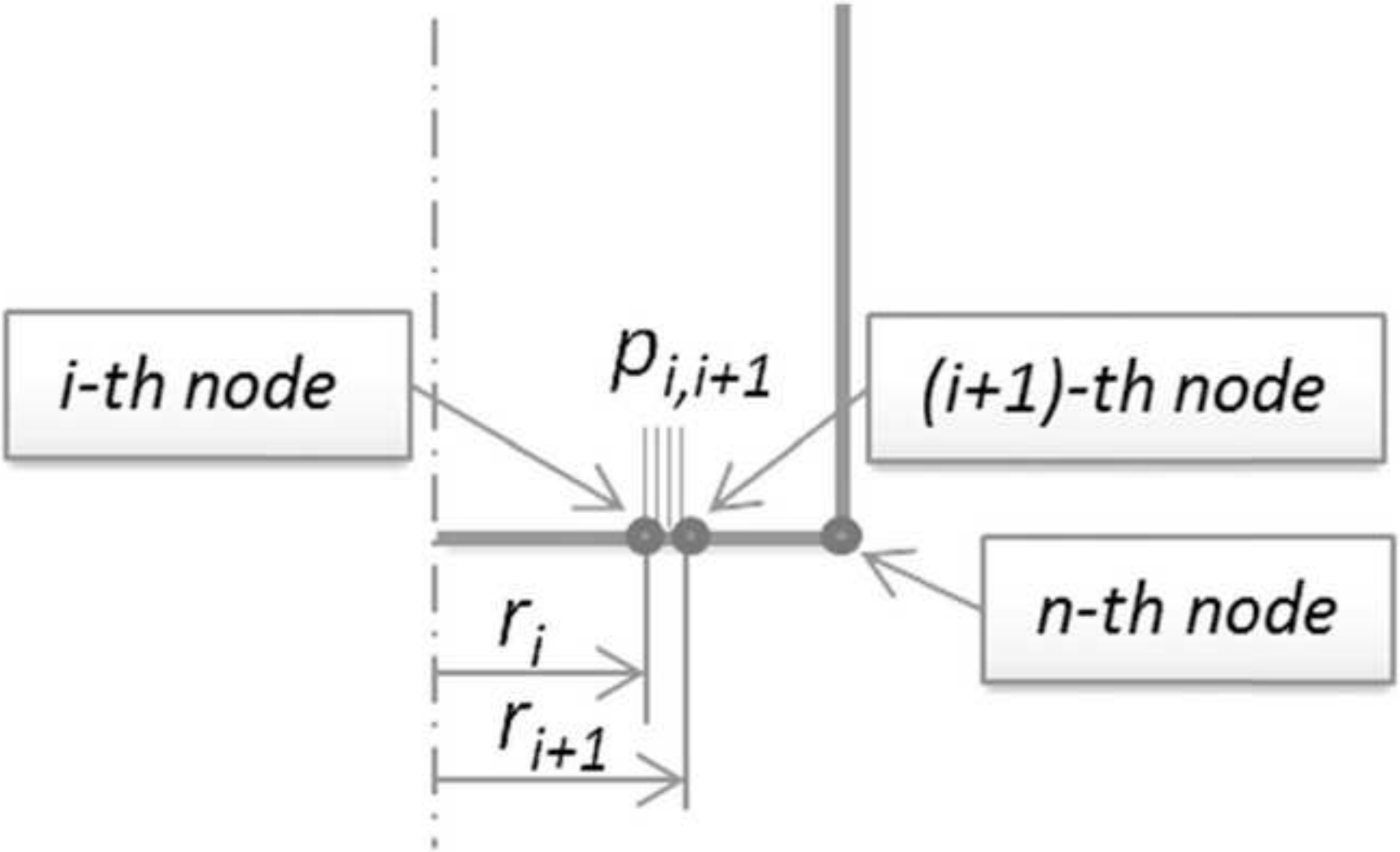

Figure_15
Click here to download high resolution image

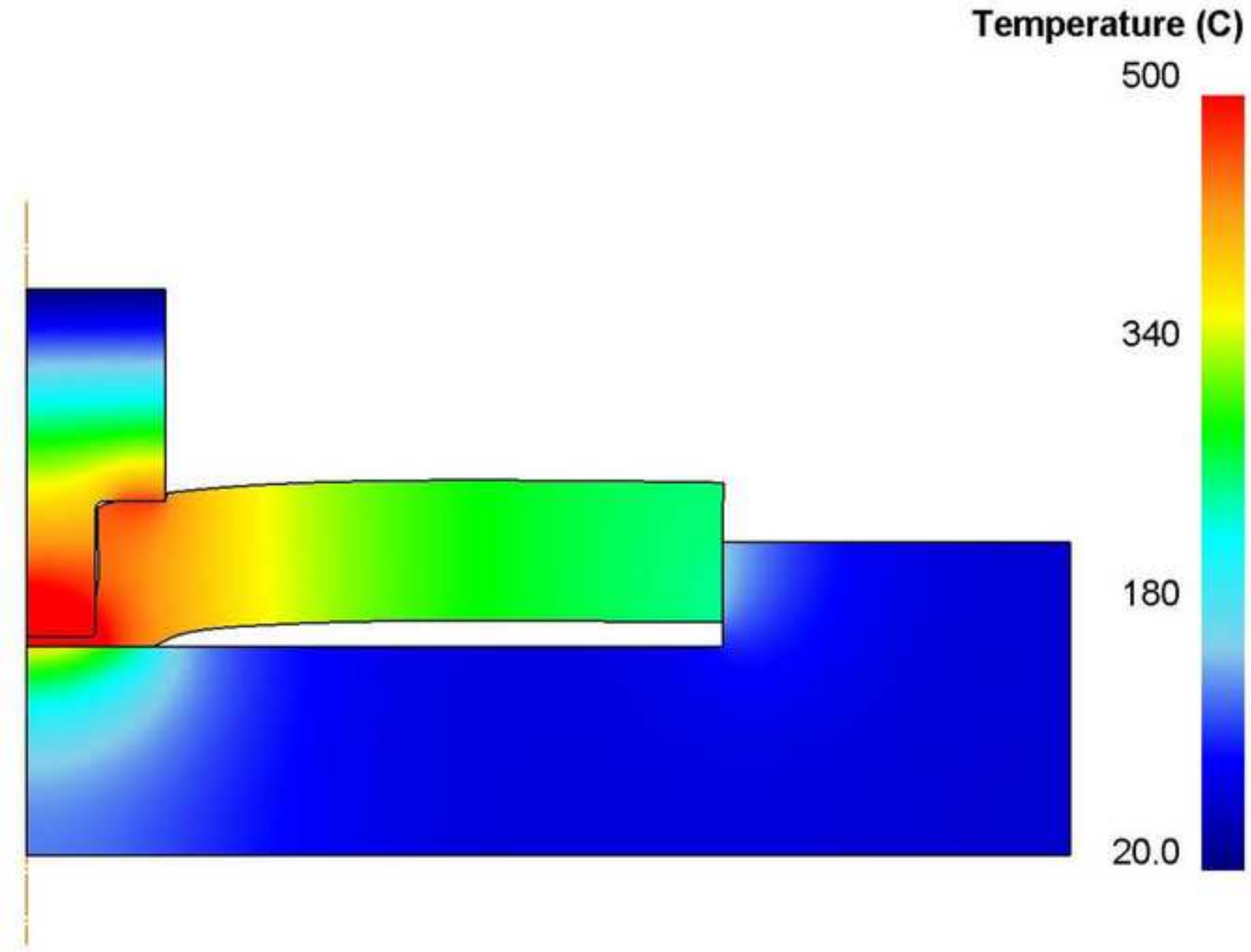

Figure_16a
Click here to download high resolution image

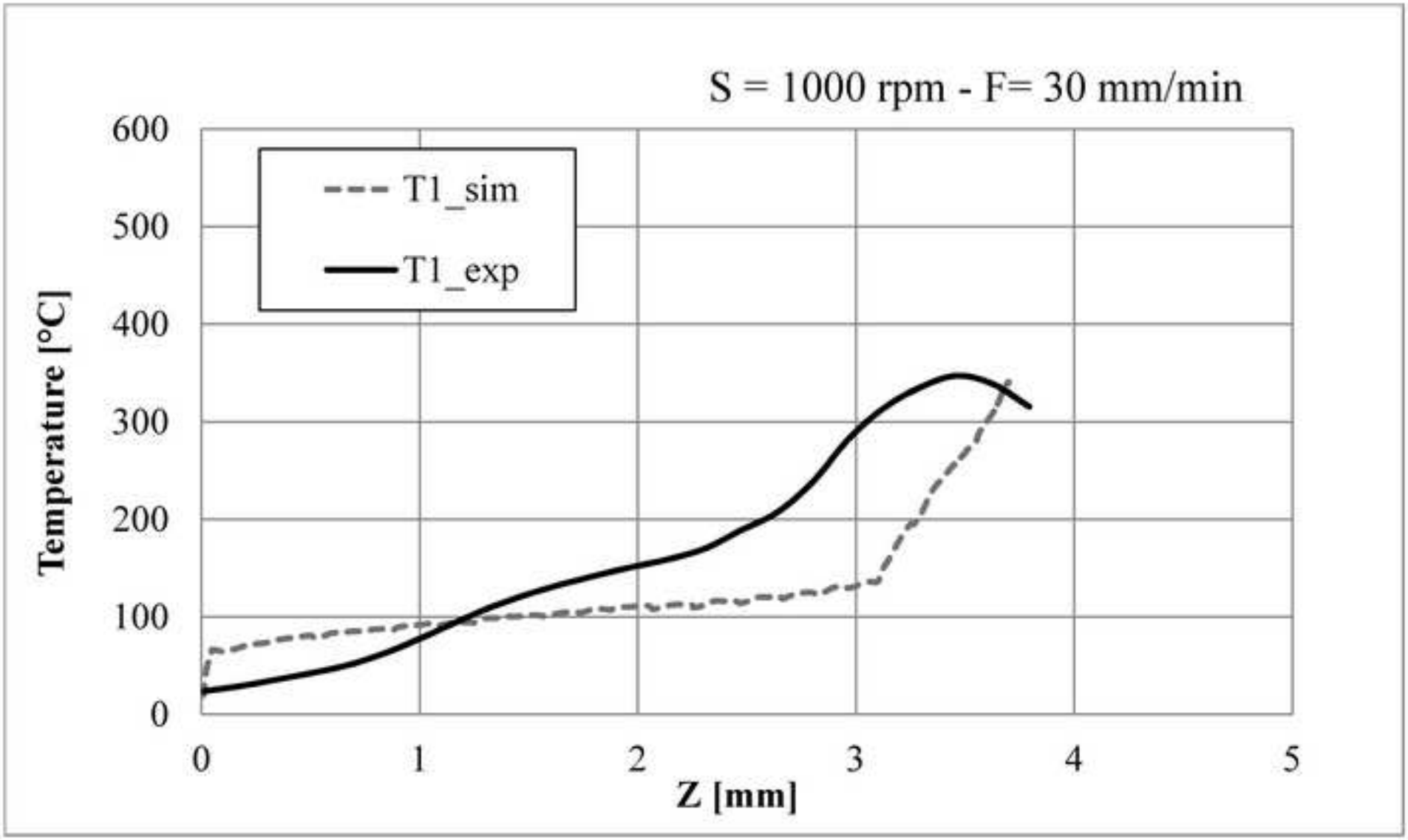

Figure_16b
Click here to download high resolution image

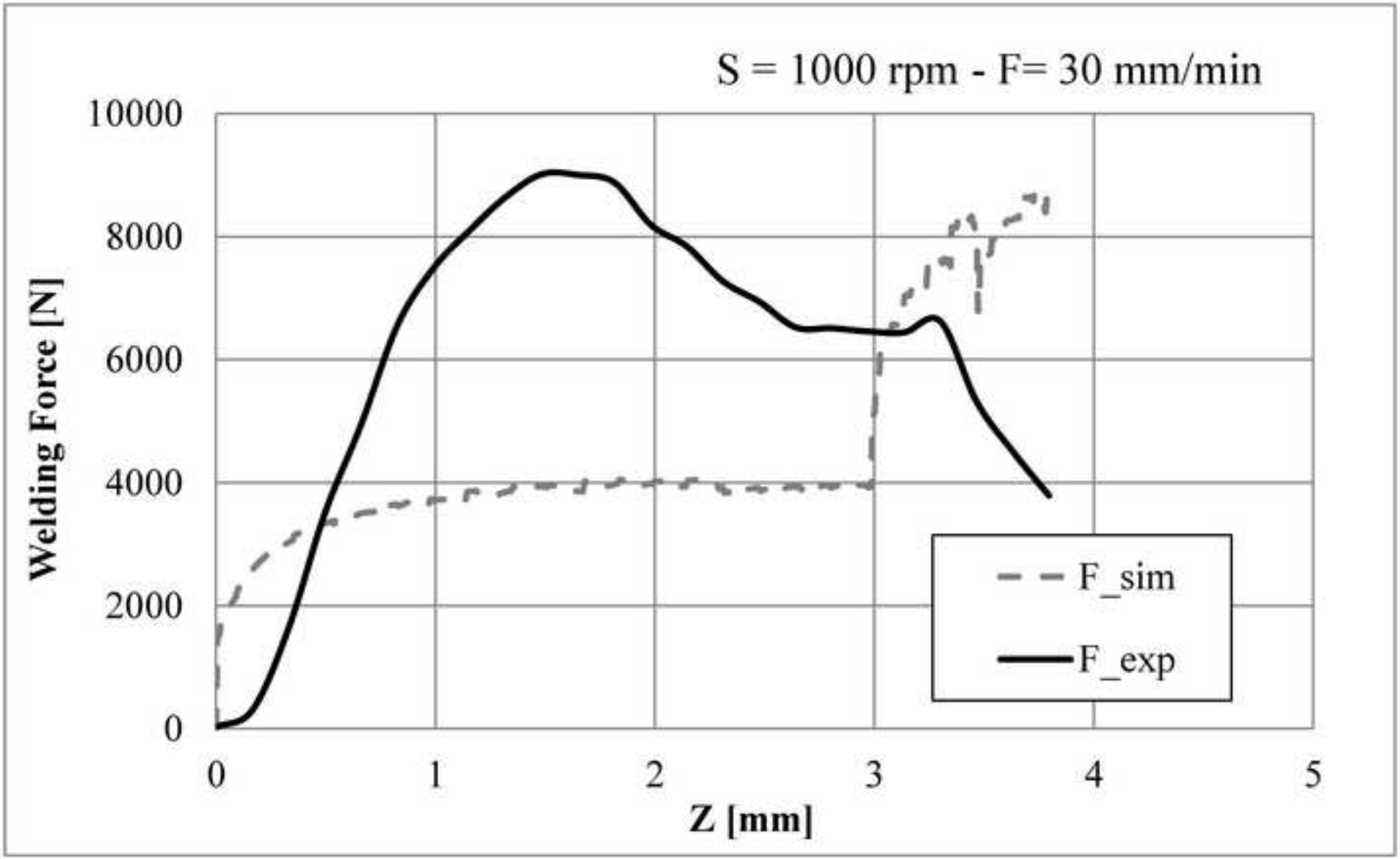

Figure_16c
Click here to download high resolution image

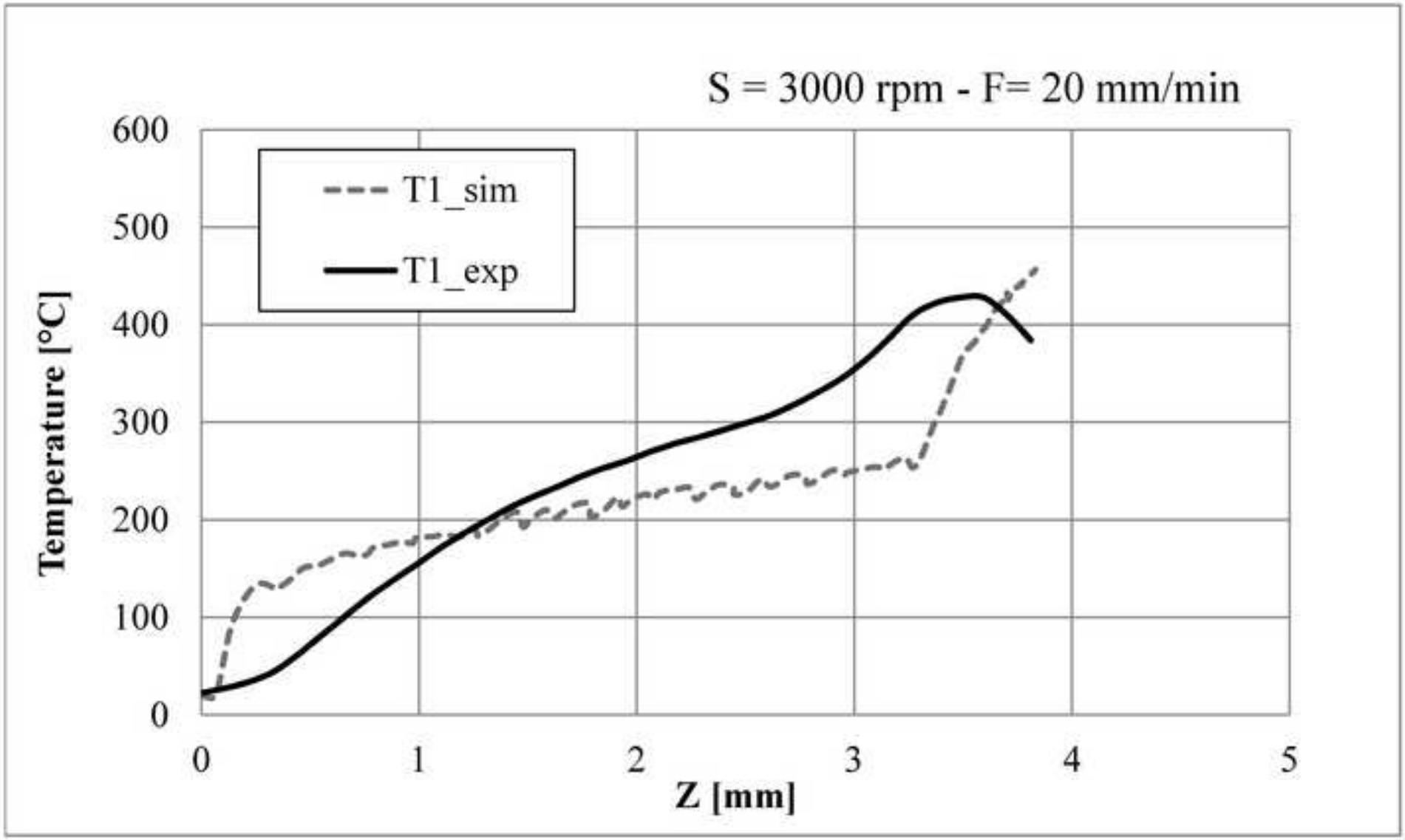

Figure_16d
Click here to download high resolution image

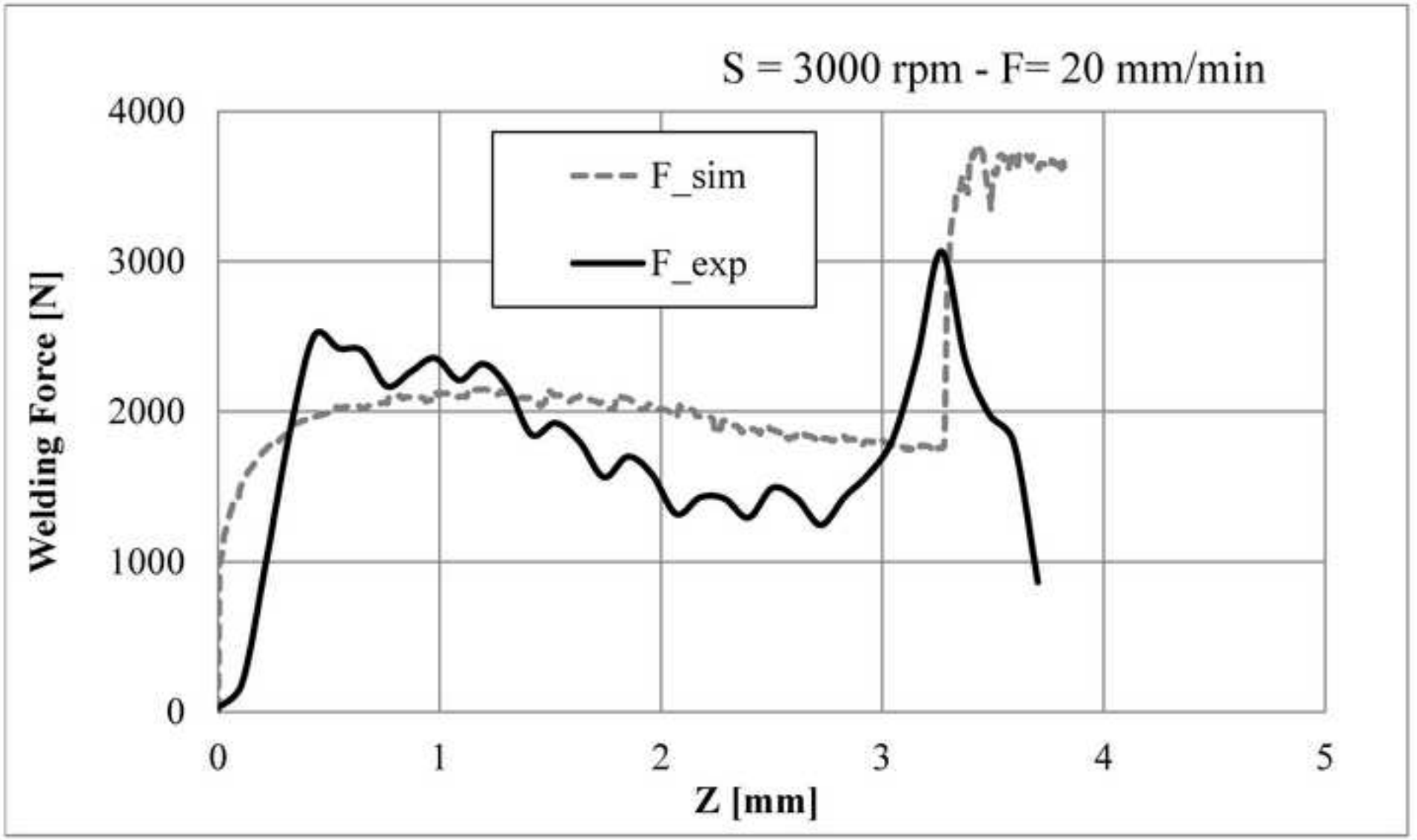

Figure_16e
Click here to download high resolution image

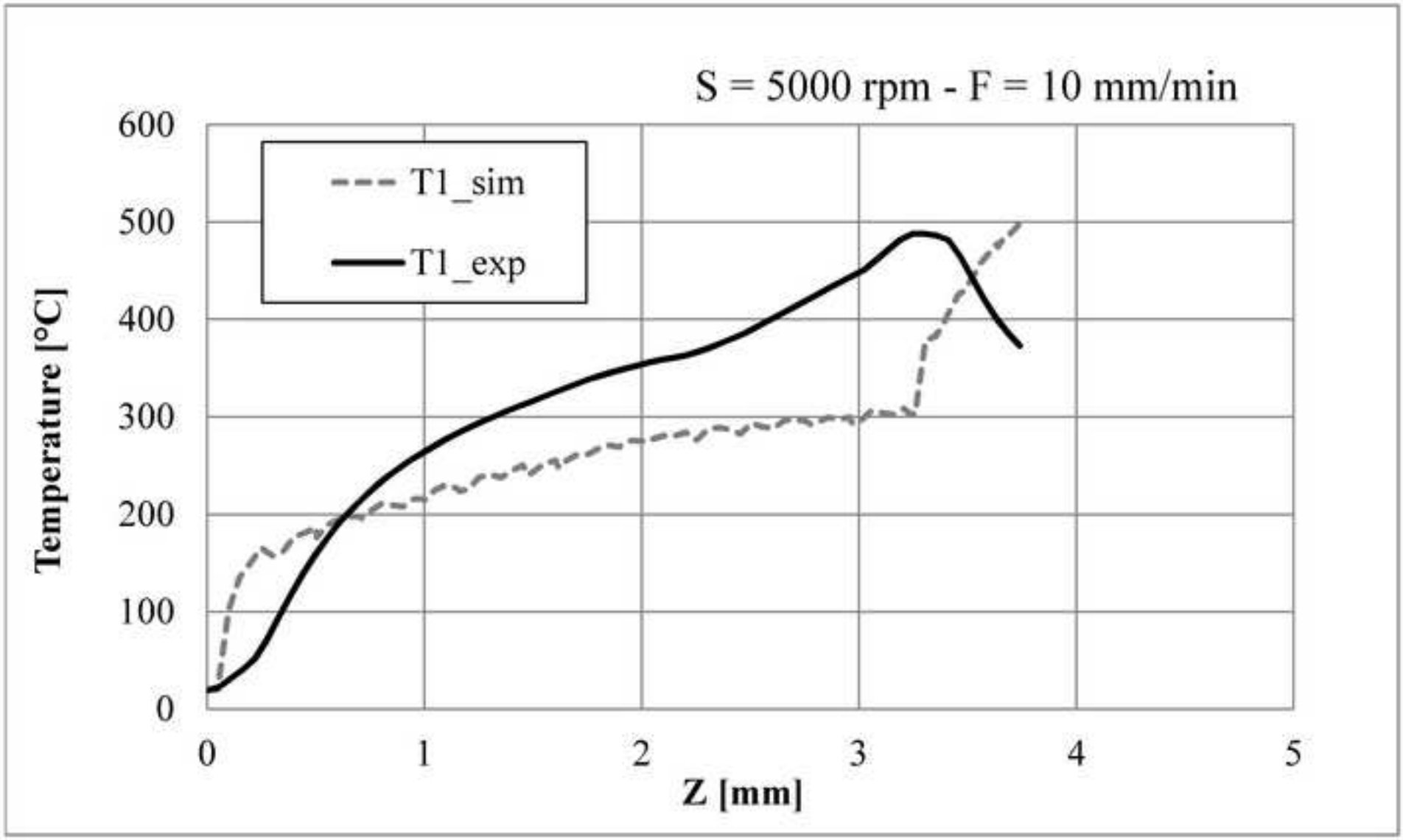

Figure_16f
Click here to download high resolution image

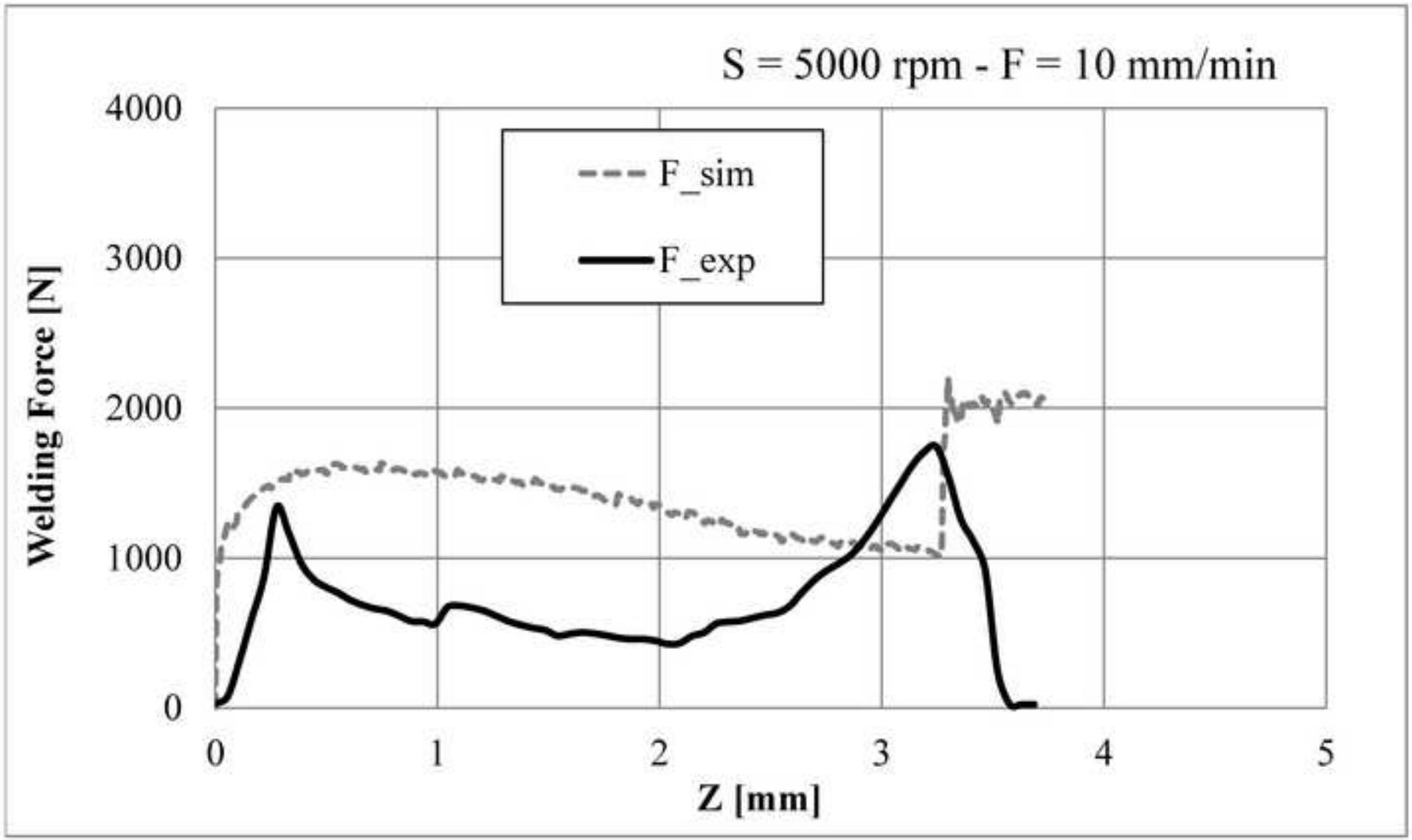

Figure_17
Click here to download high resolution image

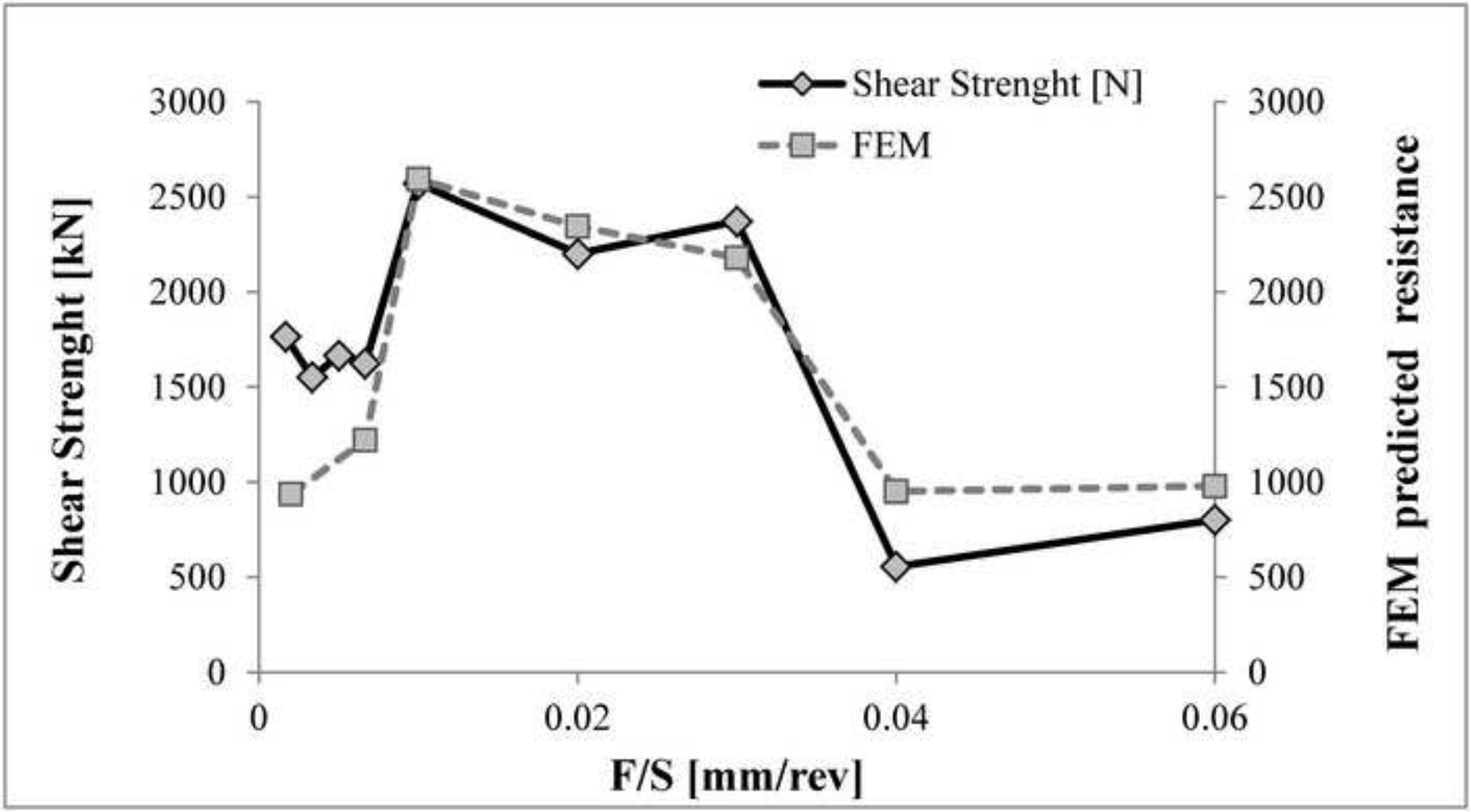

Table_01

Rotational Speed (S) [Rpm]	Feed Rate (F) [mm/min]	Plunging Depth (Z) [mm]	Dwell Time (t) [s]
1000	30	3.7	1
1000	20	3.7	1.5
5000	10	3.7	1
3000	20	3.8	0.5
5000	30	3.7	1
3000	30	3.7	1.5
3000	20	3.7	1
1000	20	3.6	1
3000	10	3.7	1.5
5000	20	3.8	1
1000	20	3.7	0.5
3000	20	3.7	1
3000	10	3.8	1
3000	30	3.8	1
3000	10	3.7	0.5
3000	20	3.8	1.5
5000	20	3.7	1.5
5000	20	3.7	0.5
3000	20	3.7	1
1000	20	3.8	1
1000	10	3.7	1
3000	20	3.6	1.5
3000	30	3.6	1
3000	30	3.7	0.5
3000	10	3.6	1
5000	20	3.6	1
3000	20	3.6	0.5

Table_02

Rotational Speed (S) [Rpm]	Feed Rate (F) [mm/min]	Plunging Depth (Z) [mm]	Dwell Time (t) [s]
500 – 1000 – 3000 – 6000	10 – 20 - 30	3.6 – 3.7 - 3.8	0.5 – 1.5

Table_03

	P-value					
Source	Welding force	T1	T2	T3	T4	T5
S	0	0	0	0	0	0
F	0	0	0	0.022	0.027	0.006
Z	0.036			> 0.05		
t	> 0.05			> 0.05		
S*S	0			> 0.05		

Table_04

Source	P-value
S	0
F	0.001
Z	0
t	0.001
S*Z	0.001